Elastin-like Polypeptide Linkers for Single Molecule Force Spectroscopy

Wolfgang Ott[a,b,⊥], Markus A. Jobst[a,⊥], Magnus S. Bauer[a], Ellis Durner[a], Lukas F. Milles[a], Michael A. Nash[c,d], Hermann E. Gaub[a,#]

[a] Lehrstuhl für Angewandte Physik and Center for NanoScience, Ludwig-Maximilians-Universität München, 80799 Munich, Germany.

[b] Center for Integrated Protein Science Munich (CIPSM), Ludwig-Maximilians-Universität München, 81377 Munich, Germany.

[c] Department of Chemistry, University of Basel, 4056 Basel, Switzerland.

[d] Department of Biosystems Science and Engineering, Swiss Federal Institute of Technology (ETH Zurich), 4058 Basel, Switzerland.

[⊥] These authors contributed equally to this work

[#] Corresponding author: gaub@lmu.de

KEYWORDS: single molecule force spectroscopy, elastin-like polypeptides, biopolymer spacer, sortase coupling, protein ligation

Author Contributions:
WO: experiment design, sample preparation, measurements, data analysis, writing of manuscript; MAJ: experiment design, data analysis, writing of manuscript; MSB: data analysis; ED: sample preparation; LFM: data analysis; MAN: experiment design, writing of manuscript; HEG: experiment design, writing of manuscript;

ABSTRACT

Single molecule force spectroscopy (SMFS) has evolved into a standard technique in mechanobiology and in turn benefits greatly from new discoveries and developments in biochemistry. Novel immobilization strategies for biomolecules and improved purification schemes are constantly adapted. In a majority of reported SMFS studies, polyethylene glycol (PEG) was used to anchor the molecules of interest to the surfaces. However, its well-known trans-trans-gauche to all-trans transition causes marked deviation from standard polymer elasticity models like the Worm Like Chain (WLC), particularly at elevated forces. As a result, the assignments of unfolded protein domains corresponding to their amino acid chain lengths are distorted, and zero force contour length fits of standard elasticity models to the data falsely appear longer. A solution addressing this issue is the implementation of unstructured polypeptides as linkers. Progress in cloning techniques of highly repetitive genes and post-translational protein ligation methods facilitated the access to peptide backbones as artificial spacers. We investigate the suitability of a tailored polypeptide linker focusing on the special requirements for single molecule force experiments, *i.e.* length, monodispersity, or bioorthogonal tags. Here, we report the use of elastin-like polypeptides (ELPs) as surface linkers for SMFS experiments, replacing PEG as surface immobilization anchors. Our results demonstrate that a single type of polymer backbone with the same elastic properties throughout the whole measured molecule improves data quality and facilitates data analysis and interpretation in force spectroscopy experiments. Thus, the use of all-peptide linkers opens alternative ways of modifying and immobilizing proteins for future studies.

MAIN TEXT

Single molecule force spectroscopy (SMFS), is a state-of-the-art technique in the rapidly growing field of molecular biomechanics.[1–3] New tools and methods are being developed constantly to improve ease of handling, sensitivity, reproducibility and reliability.[4,5] In parallel, the biochemical toolbox is expanded continuously, paving the way towards analysis of more complex and demanding biological systems. Improvements like the use of orthogonal binding handles,[6–9] new immobilization strategies,[10–14] and diverse sources of protein production (*i.e.* recombinant bulk expression or cell-free *in vitro* expression) along with parallel and multiplexed probing of different proteins within the same experiment are all examples of the significant technical advances that have been achieved in recent years.[15]

A key requirement to probe many different protein domains in a single experiment with highly controlled, site-specific protein geometry, is the ability to use a single cantilever over a long period of time for a large number of force scans. We found two main advances, the first of them being the improvement of geometrically defined and covalent surface tethering, and the second being the discovery and characterization of the type III Cohesin:Dockerin (Coh:Doc) interaction.[7] This protein receptor-ligand pair can withstand remarkably high forces in a SMFS assay and exhibits long term functionality, which was particularly important

for the establishment of multiplexed experiments. Coh:Doc can be used as a binding handle successfully and continuously for over 24 hours of measurement time without loss of binding activity. Datasets of typically several ten thousands of force-extension curves can easily be obtained using type III Coh:Doc, dramatically outperforming other mechano-stable interactions (*e.g.* biotin-avidin).

Being able to extend measurement time with one cantilever over several days offers the opportunity to address different proteins immobilized on different positions of the same substrate (*i.e.* protein microarrays). Over the course of a single experiment, the same cantilever can be used to interrogate several protein spots on a surface, and record thousands of traces from each spot to achieve statistical significance. This leads to large data sets, and requires the use of sophisticated algorithms to identify and extract specific and single molecular interactions among a vast number of traces with background signal. Empty traces, multiple interactions in parallel, and non-specific interactions must all be filtered out of the data set. Most importantly, these algorithms have to separate the different contributions stemming from the heterogeneous stretching behavior of the mixed PEG-protein polymer backbone.

When performing SMFS in an elevated force regime, additional challenges arise: a conformational transition of PEG occurs to a large extent in a force range of 100-300 pN, resulting in a linear regime in the unfolding traces.[16–18] In aqueous buffer, PEG is stabilized by water molecules in a trans-trans-gauche conformation. With rising force on the polymer, the occupancy of conformations is shifted from trans-trans-gauche to all-trans, effectively increasing the net polymer contour length. Analysis methods such as detecting contour length increments and fitting standard elasticity models to the data within said force range are therefore compromised and would, for a quantitative description require novel heterogeneous elasticity models. For many of the specifically pulled experiments done so far, this was only a minor issue, since binding handles besides type III Coh:Doc, dissociated below this regime. For probing protein unfolding and receptor-ligand unbinding in a high force regime, however, this issue becomes significant and noticeable in the traces.

In this study we investigate the feasibility of biological protein polymers to circumvent this problem. We selected the well-characterized elastin-like polypeptides (ELPs) as a suitable candidate for this purpose. The progression of cloning techniques of repetitive genes set a basis for precisely defined protein polymers.[19–22] It opened the ability to design, produce and purify protein spacers for single molecule experiments that exhibit complete mono-dispersity, a key advantage compared to other synthetic polymers like PEG. Furthermore, ELPs can be produced with N-/C-terminal protein ligation tags, which can be used for specific and orthogonal surface chemistry in SMFS sample preparation. ELPs are synthetic biopolymers derived from tropoelastin domains and are composed of a repetitive amino acid heptamer ‘Val-Pro-Gly-Xaa-Gly’.[23] Xaa is a guest residue, which can be any amino acid apart from proline. The guest residue influences the hydrophobicity of the protein and therefore impacts the reversible lower critical solution temperature, a phase transition point. At this environment-dependent cloud point, ELPs change their conformation and precipitate, resulting in clouding of the solution. As ELPs are intrinsically disordered proteins they are suitable as spacer or linker molecules.[24] They do not fold into well-defined domains, but rather remain flexible. We therefore hypothesized that ELPs would be an ideal choice for surface passivation and site-specific immobilization for nanomechanical systems. The bulky,

but still flexible features of ELPs seem to inhibit non-specific protein binding to the surface, while enabling ligation of other proteins due to their high degree of accessibility of N- or C-terminally attached tags. Advances in post-translational protein ligation methods have made it possible to move from organic chemical conjugation methods towards enzyme-mediated protein immobilization, for example utilizing Sortase A or Sfp.[14,25] Both enzymes catalyze a sequence- and site-specific reaction, yielding a uniform protein orientation on a surface.

Compared to the commonly used PEG linkers, ELPs have several advantages for use in SMFS assays. Since they are expressed recombinantly in *Escherichia coli (E. coli)*, their production is easily scaled up, resulting in lower costs compared to commercially available heterobifunctional PEGs. More importantly, recombinantly produced ELP linkers are inherently monodisperse, and can be produced in the laboratory over a wide range of molecular weights and compositions. Monodisperse ELP linkers fused directly to a protein of interest allow for complete control of the lengths of a nanomechanical system from the surface up to the force transducer, which is not true for the chemically synthesized PEG polymers with non-negligible polydispersity.

Another drawback of PEG as high force spacer are its complex elastic properties which differ significantly from those of unfolded proteins and therefore require a heterogeneous elastic model elasticity of the unfolded protein backbone in series with the PEG, which complicates data analysis and automated search routines. PEG is a highly flexible polymer with a low persistence length, while peptide bonds have restricted degrees of freedom, which alter the stretching behavior. The shift of the proportion of PEG linker length to protein backbone length ultimately affects the overall elastic response to force, by altering the measured net persistence length over the course of a polyprotein unfolding experiment when analyzed with a homogeneous polymer elasticity model.

ELPs have already been the subject of AFM studies in prior work, for example, to support theoretical predictions about the behavior of these polymers above and below their cloud point and to contribute to insights into their elasticity.[26–28] This study, however is carried out far below the cloud point so that the ELP-inherent intermolecular interactions are negligible. In contrast to prior studies, we employ ELPs as spacer molecules with other protein domains attached. Our results show that particularly at elevated force regimes, ELPs provide several attractive features making them highly suitable as protein spacers for force spectroscopy.

This study offers an attractive substitute of the established PEG spacers by using all-protein based ELP anchors. This immobilization strategy provides precise control over the elastic properties of a multi-component protein mechanical system linked between the glass surface and the force transducer. Our approach transfers advances in smart polymer research towards SMFS experiments and investigates the feasibility of an alternative surface anchoring strategy.

RESULTS AND DISCUSSION

State of the art SMFS experiments employ site specific pull down strategies. Typically PEG linkers with an *N*-Hydroxysuccinimide (NHS) group are linked to an amino silanized surface. The other end of the PEG contains a reactive group for protein immobilization, which in most cases is a thiol reactive maleimide group. **Figure 1 A** illustrates a typical SMFS experiment. Proteins anchored to a functionalized glass surface are probed by the corresponding receptor fusion protein covalently linked to the cantilever tip. A typical unfolding curve recorded at constant speed is shown in **Figure 1 B**. After the Coh:Doc complex is formed by contacting the cantilever with the surface, force is applied by retracting the base of the cantilever. The signal is detected by a quadrant photodiode with a laser beam that is reflected off the backside of the cantilever. Bending of the cantilever is translated into a differential voltage output of the photodiode amplifier. With retraction of the cantilever at constant speed, first the polymer linker is stretched **(Figure 1 B, I)**, then the weakest component in the assay unfolds. In this case two carbohydrate binding module (CBM) are unfolding consecutively **(Figure 1 B, II and III)**. Finally the force raises to a level where the receptor ligand pair dissociates and it subsequently drops to zero **(Figure 1 B, IV).** Now the cantilever is able to probe a new molecule on a different spot of the surface. In order to quantify the hidden lengths of the folded proteins that are released by the unfolding, a multilevel sorting algorithm identifies characteristic unfolding pattern taking into account the unfolding force and the gained increment in contour length of the peptide backbone of the CBM fingerprint domains.[29]

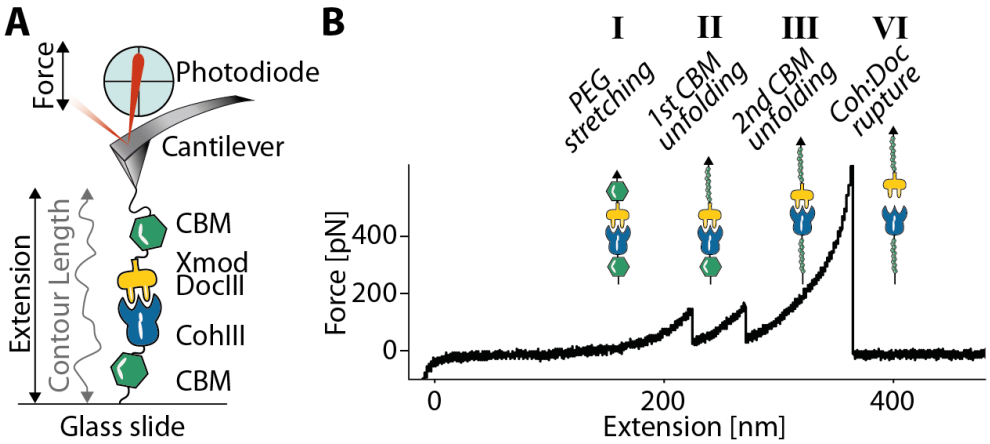

Figure 1 (A) SMFS configuration: Cantilevers are functionalized with CBM-Xmod-DocIII fusion proteins. Glass slides are modified with CohIII-CBM constructs. **(B)** A typical SMFS unfolding trace. The approached cantilever enables the Cohesin:Dockerin complex formation at zero extension. With the retraction of the cantilever, the biological system is stretched mechanically. **I)** First, the spacer molecules are fully extended and stretched. **II,III)** the weakest links in the chain, usually the fingerprint domains (here: CBM) are unfolded. **IV)** Finally, the Cohesin:Dockerin complex dissociates under force and the unfolded CBM domains can refold after the force drop. The cantilever is now able to probe a new molecule on the surface.

For this study, multidomain proteins with CBM domains as force spectroscopy fingerprints and the robust type III Coh:Doc interaction from *Ruminococcus flavefaciens* (*R. f.*) as a mechanical handle were produced.[7] The comparison of PEG with ELP linkers was carried out by cloning and recombinantly expressing two different ELPs both with 120 nm theoretical contour length (ELP_{120nm}, assuming 0.365nm per amino acid).[30] One ELP construct contained an N-terminal Sortase-tag ('GGG') and a C-terminal cysteine. The other ELP linker had the Sortase-tag at its C-terminus ('LPETGG') and a cysteine at the N-terminus. Two identical bioconjugation routes were used to attach ELP or PEG linkers to both cantilever and glass surface (**Figure 2**). To achieve the most direct comparison, 15 kDa PEG linkers of similar contour lengths (~ 120 nm) were used. For PEG experiments, 15 kDa NHS-PEG-Maleimide was immobilized onto an amino silanized glass slide (PEG_{120nm}). The maleimide groups of the PEG reacted with a GGGGG-cysteine peptide, leaving the Sortase N-tag available for subsequent derivatization. For ELP experiments, a small-molecule crosslinker (sulfosuccinimidyl 4-(N-maleimidomethyl)cyclohexane-1-carboxylate), sulfo-SMCC), which added negligible contour length (0.83 nm) to the system was first immobilized onto amino silanized glass, followed by coupling with GGG-ELP_{120nm}-Cys. Both strategies resulted in the Sortase N-tag being available for conjugation *via* Sortase-mediated enzymatic ligation. The protein of interest (CohIII-CBM-LPETGG) was linked by Sortase A to ELP or PEG (**Figure 2**). The same was done for the cantilever, except GGG-Xmod-DocIII being conjugated by Sortase A to Cys-ELP_{120nm}-LPETGG or to PEG_{120nm} coupled Cys-LPETGG. Our enzyme-mediated protein immobilization approach has the advantage of site-specific linkage and results in a homogeneous orientation of proteins on the surface. Such uniformly immobilized proteins lead to a well-defined propagation of the applied force through the molecular complex under investigation and as a result to a narrow and well defined distribution of the measured force-extension curves.

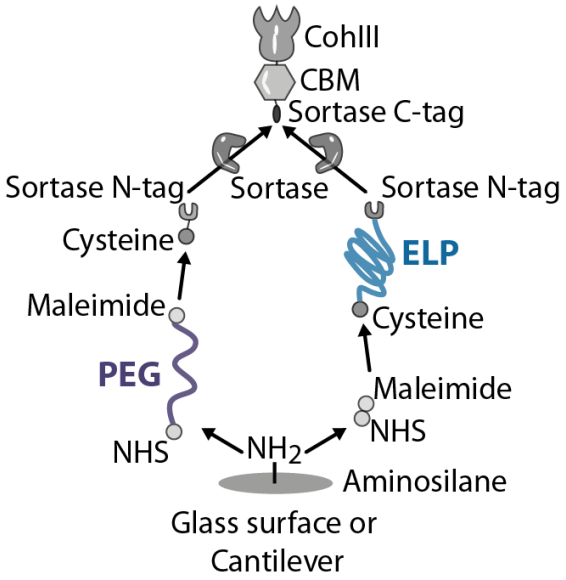

Figure 2: Comparison of immobilization strategies. Strategies of biomolecule immobilization: for standard immobilization with PEG spacers, NHS chemistry is used to link to amino silanized surfaces. Protein constructs are then coupled *via* cysteine-Sortase tag peptides to the maleimide end-groups on the PEG spacers. For immobilization with ELP linkers, only a small molecule NHS-maleimide crosslinker with a negligible contour length of 0.83 nm was used to couple cysteine-ELP spacers with a Sortase-tag to the amino silanized surface. In both cases, fusion proteins of interest, consisting of CBM fingerprint domains and mechanostable pulling handles, were enzymatically coupled to the

immobilized molecules on the surface in a subsequent step. Depicted is the functionalization of the glass surface with CohIII. The functionalization of the tip with DocIII follows the identical scheme.

The ELPs in this study contained functional tags at their N- and C-termini for surface chemistry, which also ensured that only fully translated constructs were coupled. Our AFM experiments with ELPs as linkers showed a higher percentage of single molecule unfolding traces, which may be attributed to the bulky character of the ELPs. They provide a less dense surface immobilization of the biomolecules of interest when compared to PEG-based immobilization. This behavior is advantageous since too high surface densities frequently cause multiple interactions between surface- and cantilever-bound molecules in SMFS experiments (**Supplemental Figure S8**). Multiple interactions are generated, when more than one receptor-ligand interaction is recorded in parallel in a single SMFS force distance trace. The interwoven unfolding and unbinding events hamper data interpretation (**Supplemental Figure S9**). Efficient passivation of glass surfaces against nonspecific adhesion of proteins requires a dense PEG surface layer, to prevent proteins from diffusing towards and sticking to the glass surface. Approaches like titrating functional (*i.e.* maleimide end-groups) with non-functional (*i.e.* CH_3 end-groups) PEG, or changing the concentration of binding agents or proteins of interest can improve the process. In our experience, surface immobilization with ELP instead of PEG linkers leads to better passivation of the surface and a higher percentage of single molecule traces, without the need for any titration of functional and non-functional linkers.

All unfolding traces were presorted by an automated routine, selecting for single interactions that display two consecutive CBM unfolding events, followed by a manual deletion of obviously erroneous curves (typically 10 %), *e.g.* caused by baseline drift.[7,29] PEG unfolding traces showed wildly varying initial extensions prior to the first CBM unfolding event. We interpret this to be caused by the non-negligible polydispersity of PEG, as we did not observe multiple discrete populations with ELP experiments. The intrinsic monodispersity of ELP molecules is another clear advantage. Since they are produced recombinantly in *E. coli* cells and capped terminally with functional tags *in vivo*, only the full length constructs are functional. Additionally, ELPs were purified with inverse transition cycling (ITC), a method developed for ELP purification based on their reversible precipitation behavior. Possibly shorter ELPs are removed during the process, since their cloud point is higher than for ELP_{120nm}. Although the polydispersity of chemically synthesized PEGs (mass distribution ~10 - 20 kDa) is sufficient for many applications, it can lead to a noticeable impact in SMFS.

Figure 3 A shows typical SMFS traces recorded with both PEG and ELP linkers and also gives examples of the shortest and largest extensions found. **Figure 3 B** shows a histogram of all extensions at which the unfolding events of the first CBM occur. For ELP, the distribution shows one peak centered at the extension, which is to be expected from the known ELP linker length. In the case of the PEG experiment however, three distinct populations are observed. This can be understood considering that at the level of single molecules a polydisperse distribution results in discrete peaks representing the corresponding lengths of the polymeric linkers involved in the experiment. The three peaks thus stem from the stochasticity of the SMFS experiment with three different PEG linker combinations. This polydispersity is clearly disadvantageous, since multiple linker length populations render data analysis more difficult. Curves cannot simply be overlaid in force-distance space, due to varying loading rates. Furthermore, for constant speed SMFS

experiments, loading rate populations in dynamic force spectra get broadened due to the probabilistic nature of the thermally driven rupture events. We attribute the width of the peaks to geometry effects of the anchor sites on the cantilever tip, as well as off-axis binding to molecules on the surface.

It should also be noted that the PEG data show a softer surface indentation of the tip into the polymer brush than the ELP data, as of the curvature at the beginning of each trace. A harder surface like in the case of the ELP experiments requires less indentation force to reach the linear regime after the initial soft indentation. For calibrating the inverse optical lever sensitivity this is advantageous from a practical point of view.[31]

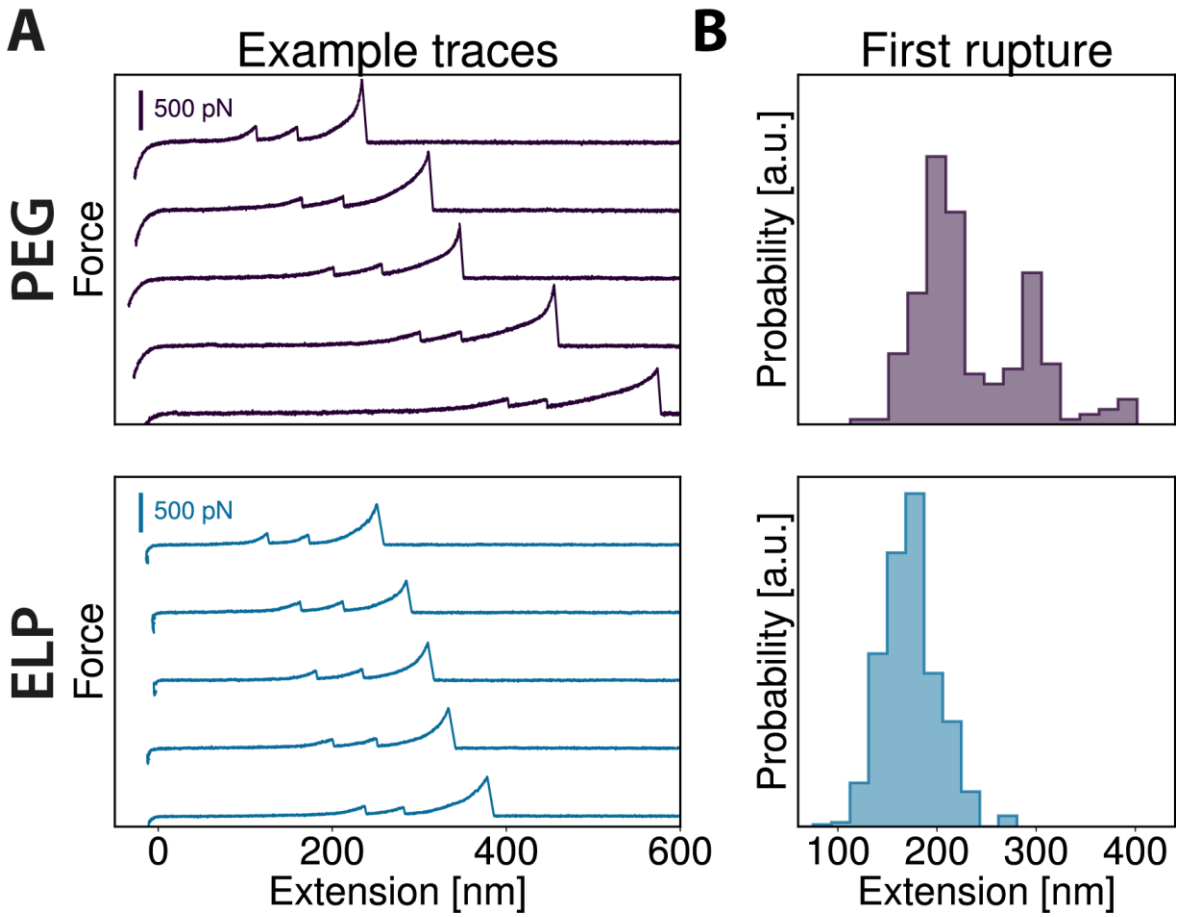

Figure 3: Comparison of dispersity of PEG and ELP linkers. (A) typical force-distance traces. In the PEG linked experiment (purple), the unfolding events occur at widely spread different absolute distance ranges, whereas with ELP linkers (blue), there is only a single distance regime. **(B)** histograms of the first CBM unfolding event of each whole data set (PEG: N=219; ELP: N=521). Due to the polydispersity of the PEG linkers, for PEG experiments, three discrete populations with different extensions are clearly visible, for ELP only one. In both cases, anchor geometry on cantilever tip and glass surface determine the shape of the populations.

In this study we hypothesized that by replacing synthetic PEG linkers with biological ELP linkers, and thereby having a single type of polymer backbone throughout the mechanical system, better defined elasticity properties for the recording of force curves would be

achievable. The persistence lengths of ELP peptide backbones should be comparable to those of unfolded protein domains, since they both consist of the same type of peptide bonded polymer chains. This match in persistence length should be advantageous compared to PEG, which contains repeats of ethylene oxide groups with lower stiffness. Accurate description of the mechanical system under investigation by elasticity models plays a crucial role determining characteristic parameters like persistence lengths and contour length increments.

Previous studies had shown, that at forces below 100 pN the PEG elasticity may satisfyingly be described by the standard elasticity models.[16] In a systematic study in this force range we compared ELP and PEG linkers and corroborated these earlier results. The data and a thorough discussion thereof are given in the supplement (see particularly **Supplementary Figure S10**).

At elevated forces however, stretching of PEG through its conformational transition causes marked deviations from ideal polymer behavior. In aqueous ambience, water molecules bridge by hydrogen bonding to two adjacent oxygen groups in the PEG backbone. By this means, they stabilize a trans-trans-gauche configuration with a binding energy of around 3 kT. When the polymer is stretched, the subunits of the backbone are forced increasingly into the slightly longer all-trans configuration and the bound water molecules are released. This conformational change, which contributes prominently to the polymer elasticity in the force range of 100 to 300 pN, causes an increase in the measured net contour length of the polymer backbone.[16,17]

Figure 4 A shows assemblies of multiple data traces of PEG and ELP linked proteins (‘master curves’), respectively. A recently introduced WLC approximation model[32] with a quantum mechanical correction for backbone stretching at high forces[33] (qmWLC) was fitted to the traces with fixed persistence length of 0.385 nm.
In the case of PEG linked proteins, a pronounced linear regime between 100 and 300 pN is visible in the last stretch at elevated forces. As a consequence, the qmWLC cannot model this polymer correctly. ELPs do not show such a conformational change to this extent, and therefore the elasticity model fits satisfyingly. An approach to let the persistence length also be a free fit parameter is shown in **Supplemental Figure S11**, but resulted in a non-physical compensation of the gauche-trans conversion by this entropic elasticity parameter and thus gave largely unrealistic values for the contour length increment. **Figure 4 B** shows details of the last stretch before the Coh:Doc dissociation, highlighting the difference between PEG and ELP linkers. Two separate fits in the respective low and high force regimes illustrate the differences in polymer length before and after the transition. ELPs were also reported to have a force-induced conformational change, in this case based on proline cis-trans isomerization, that also extended the contour lengths.[27,34] Not at least the low number of prolines in the overall sequence (every 5th amino acid) in the ELP motif renders this effect much smaller compared to the PEG conformational change, and will be camouflaged by signal noise in typical experiments with proteins. **Figure 4 C** shows the transformation into contour length space with the qmWLC model. A kernel density estimate (KDE) is plotted (gaussian kernel, bandwidth of 2.5 nm) to the distributions of the unfolding events (2x CBM, Coh:Doc dissociation). In case of PEG immobilized proteins, the KDE-contour length distribution shows several peaks, because of the failure of the model to describe the force response of the polymer accurately. Determining the contour length increments between the

peaks of the KDE proves problematic even for this relatively simple exemplary case of two large fingerprint unfolding events and a receptor ligand dissociation. Smaller unfolding steps or even folding intermediates as substeps would be even harder to pinpoint and measure. In the case of ELP immobilized proteins, only three distinct peaks appear, with much clearer transformed data populations.

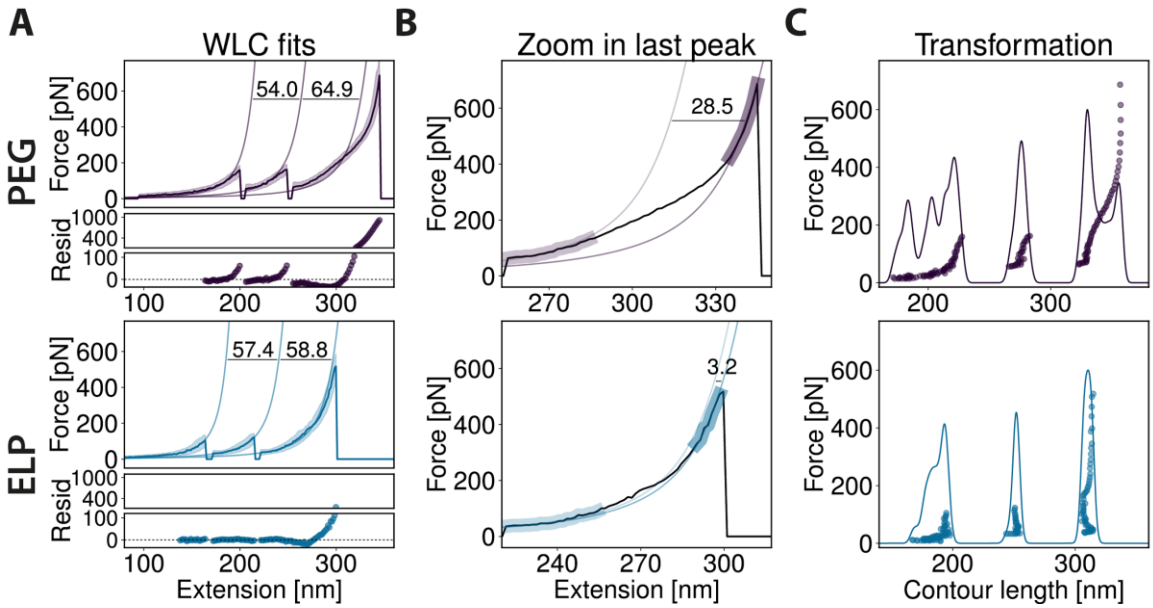

Figure 4: Elasticities of PEG and ELP linkers. (A) superposition of multiple protein unfolding curves ('master curves') from SMFS experiments with PEG (purple, N=73) and ELP linkers (blue, N=151). The lower plots of each graph in panel A show the residuals of each WLC fit. Note that the residual plots are split in two subranges from -35 to 120 pN and from 120 to 1100 pN. The applied WLC model is extended by *ab initio* quantum mechanical calculations to correct for the enthalpic stretching of the polymer backbone[33] and is fitted to the data with a fixed persistence length. The fits show that the stretching behavior of the mixed polymer system (PEG linkers) deviates markedly at elevated forces from the predictions of the elasticity model, whereas the ELP curves agree very well. **(B)** the final stretch of the Coh:Doc rupture event, fitted with the WLC models with two different contour lengths in the lower and upper force regime. The PEG molecules undergo a conformational transition[16], resulting in different contour lengths for each force regime. For ELP molecules, a comparable transition was reported[27,34], which apparently contributes to a much lower extent, so that SMFS experiments are much less affected. The differences in fitted contour length between the two fits are 28.5 nm for PEG linkers and 3.2 nm for ELP linkers. **(C)** contour length transformations[29,35] of PEG and ELP master curves (purple and blue points). Ideally, the transformation results in data points aligning on vertical lines, where each line represents an energy barrier position for each stretching regime between two peaks in force-extension space. A KDE (gaussian kernel, bandwidth: 2.5 nm) was calculated for the transformed data. The ELP dataset shows the expected three peaks for the three unfolding and dissociation events, whereas the PEG data exhibit an irregular distribution with several more maxima.

CONCLUSION

PEG linkers have successfully been employed in numerous studies to anchor biomolecules of interest for SMFS. In the low force regime (below 100 pN) the extended WLC model describes their elastic properties with sufficient accuracy for the majority of applications. For higher forces, however, the conformational transitions in the PEG backbone would require

an extended model for a convincing description.[16] Moreover, the inherent polydispersity of the PEGs, together with their complex elasticity make them less favorable linkers for SMFS.

The ELP-based linkers however, have proven in our studies to be improved candidates for surface immobilization and passivation purposes in single molecule force experiments. ELPs are monodisperse and flexible linkers, and readily allow for direct, site specific tethering. We showed that these features lead to more accurate measurements of contour length increments in poly-protein force spectroscopy data. A well-established elasticity model suffices for the data analysis.
The ELPs investigated here are only one formulation of the vast variety of smart polymer linkers that could be utilized in SMFS experiments. Further studies are required to evaluate completely non-structured, non-proline containing protein linkers and their suitability for SMFS studies, because the amino acid side chain composition may affect the persistence length[36,37] and even raise non-entropic behavior. Biotechnological characteristics, *i.e.* recombinant production and purification are as important as the biophysical requirements, which renders the easily produced ELPs particularly attractive. Other smart polymers should be similarly accessible to perform as suitable alternatives. Studies on smart polymers as tethers for SMFS experiments might also help to develop environmentally responsive surfaces, which potentially open the way towards new and exciting applications in nanobiosciences.
In this work, ELPs as surface anchors enabled straightforward attachment of protein domains with Sortase A, and can easily be combined with other orthogonal peptide or protein ligation methods. The right choice of surface tethers helps administering accuracy and resolution to single molecule force spectroscopy and related scientific fields. Particularly, this method could not only be applied to enhance SMFS studies with purified proteins on functionalized surfaces, but also, when only the force probe is modified and subsequently used to measure on artificial membranes or cell surfaces. The approach presented here can easily be applied by standard molecular biology equipped laboratories to streamline the procedure and improve data quality for resolving even smaller features accurately.

MATERIALS AND METHODS

All reagents were at least of analytical purity grade and were purchased from Sigma-Aldrich (St. Louis, MO, USA) or Carl Roth GmbH (Karlsruhe, Germany). All buffers were filtered through a 0.2 µm polyethersulfone membrane filter (Nalgene, Rochester, NY, USA) prior to use. The pH of all buffers was adjusted at room temperature.

A 300 amino acid long ELP was the basis for the AFM linker constructs used in this study, the underlying cloning and protein purification procedure of the ELP is described in detail elsewhere.[19] The ELP sequence was: $[(VPGVG)_5\text{-}(VPGAG)_2\text{-}\ (VPGGG)_3]_6$ and is referred to as ELP_{120nm}.

Standard molecular biology laboratories capable of producing recombinant proteins are equally capable of expressing ELPs, since both rely on the same principles, reagents and instrumentation. With our Plasmids provided at Addgene, cloning can even be avoided and production of ELP linkers for protein immobilization can be performed right away.

Cloning

A detailed description of the cloning procedure of the constructs can be found in the Supplemental Information (**Supplemental Figures S1-S7**). ELP sequences used in this study, along with 40 nm length variants and binding handles are deposited at Addgene and available upon request (Addgene accession numbers: 90472: Cys-ELP$_{120nm}$-LPETGG, 90475: Cys-ELP$_{40nm}$-LPETGG, 90571: GGG-ELP$_{40nm}$-Cys, 90572: GGG-ELP$_{120nm}$-Cys, 91697: CohIII (R.f.)-CBM-HIS-LPETGG, 91698: GGG-HIS-CBM-Xmod-DocIII (R.f.)).

Transformation of cells

2 µl of the Gibson Assembly or ligation reaction transformed *DH5α* cells (Life Technologies GmbH, Frankfurt, Germany; 30 min on ice, 1 min at 42°C, 1 hr at 37°C in SOC medium). The cells were plated on 50 µg/ml kanamycin containing LB-Agar and incubated overnight at 37°C. Clones were analyzed with Colony PCR, clones with fragments of appropriate lengths were sent to sequencing.

Protein expression

Chemically competent *E. coli NiCo21(DE3)* (New England Biolabs, Ipswich, MA, USA) were transformed with 50 ng plasmid DNA for the expression of all constructs used in this study. Transformed cells were incubated in autoinduction ZYM-5052 media (for ELP containing constructs supplemented with 5 mg/ml proline, valine and 10 mg/ml glycine; 100 µg/ml kanamycin) for 24 hrs (6 hrs at 37°C, 18 hrs at 25°C).[38] Expression cultures were harvested *via* centrifugation (6500 g, 15 mins, 4°C), the supernatant was discarded and the pellets stored at -80°C until further lysis. Throughout the whole purification process, for ELPs containing a cysteine, 1 mM tris(2-carboxyethyl)phosphine (TCEP, Thermo Fisher Scientific Inc., Waltham, MA, USA) or 1 mM of Dithiothreitol (DTT) was added to the respective buffers. Cell pellets with proteins containing no HIS-tag were solubilized in 50 mM TRIS-HCl pH 7.5 (supplemented with cOmplete™, EDTA-free Protease Inhibitor Cocktail, Sigma-Aldrich, St. Louis, MO, USA), all other pellets in lysis buffer (50 mM TRIS, pH 8.0, 50 mM NaCl, 10 % (w/v) glycerol, 0.1 % (v/v) Triton X-100, 5 mM $MgCl_2$, DNase I 10 µg/ml, Lysozyme 100 µg/ml).

Cys-ELP$_{120nm}$-LPETGG and GGG-ELP$_{120nm}$-Cys were purified with the ITC method.[39] After resolubilization, the cells were lysed by sonication (Bandelin Sonoplus GM 70, Tip: Bandelin Sonoplus MS 73, Berlin, Germany; 40 % Power, 30 % Cycle, 2x 10 min). The cells were kept on ice during the sonication procedure. The soluble fraction was separated from the insoluble cell debris by centrifugation (15000 g, 4°C, 1 h). In a first heating step (60°C, 30 mins) of the supernatant, most of the *E. coli* host proteins precipitated. The fraction of the collapsed ELPs were resolubilized by cooling the suspension for 2 hrs to 4°C on a reaction tube roller. The insoluble host proteins were pelleted by centrifugation (15000 g, 4°C, 30 min). Further purification steps were necessary to increase the purity of the ELP solution. This was done by repeated thermoprecipitation of the ELP followed by redissolution.

The ELP solution was clouded by adding 1 M acetate buffer (final concentration 50 mM, pH 2.5) and 2 M NaCl. A heating step (60°C, 30 mins) ensured all ELPs were collapsed. A hot centrifugation (3220 g, 40°C, 75 min) was necessary to separate the high salt, low pH solution from the ELP pellet, which was resolubilized in 50 mM TRIS-HCl (pH 7.0) after discarding the supernatant. The solution was incubated for 2 hrs at 4°C to resolubilize all ELPs completely. A cold centrifugation step (3220 g, 4°C, 60 min) isolated the remaining insoluble fraction of the suspension. After decanting the supernatant, the salt concentration

was increased and pH lowered, to precipitate the ELPs again. This cycle was repeated three times, or extended if the purity of the solution was not high enough.

The constructs CohIII-CBM-HIS-LPETGG and GGG-HIS-CBM-Xmod-DocIII were expressed and lysed as described above. After the first centrifugation, the supernatant was however, filtered (0.45 µm) and applied to a HisTrap FF (GE Healthcare Europe GmbH, Freiburg, Germany). Unspecifically bound proteins on the column were removed by washing five column volumes (25 mM TRIS-HCl pH 7.8, 300 mM NaCl, 20 mM Imidazole, Tween 20 0.25 % (v/v), 10 % (v/v) glycerol). Finally, the desired HIS-tag containing protein was eluted (25 mM TRIS-HCl pH 7.8, 300 mM NaCl, 300 mM Imidazole, Tween 20 0.25 % (v/v), 10 % (v/v) glycerol).

For long term storage the protein solutions of the different constructs were concentrated (Amicon Ultra-15 Centrifugal Filter Units 10K MWCO, Merck KGaA, Darmstadt, Germany) and reduced with 5 mM TCEP overnight for constructs that contained a cysteine. The buffer of the reduced ELP solution was exchanged (Zeba™ Spin Desalting Columns 7K (Thermo Fisher Scientific Inc., Waltham, MA, USA) to 50 mM sodium phosphate, 50 mM NaCl, 10 mM EDTA, with a pH of 7.2 and 10 % (v/v) glycerol and flash frozen in liquid nitrogen in small aliquots to be stored at -80°C. All other proteins were exchanged to 25 mM TRIS-HCl, 75 mM NaCl, 5 mM $CaCl_2$ with a pH of 7.2 and supplemented with a final glycerol concentration of 20 % (v/v).

SDS-PAGE (Any kD™ Mini-PROTEAN® Stain-Free™ Gels, Bio-Rad Laboratories GmbH, Hercules, CA, USA) was employed to detect any impurities. Since ELPs could not be stained with the Stain-Free technology an Alexa Fluor® 647-C_2-Maleimide dye (Thermo Fisher Scientific Inc., Waltham, MA, USA) was incubated for 1 hr at room temperature with the ELP solution. Appropriatly diluted protein solution was mixed with 5x Loading buffer (250 mM TRIS-HCl, pH 8.0, 7.5 % (w/v) SDS, 25 % (v/v) glycerol, 0.25 mg/ml bromophenol blue, 12.5 % (v/v) 2-mercaptoethanol) and heated for 5 mins at 95°C.

Protein concentration was photometrically determined at 205 nm (Ultrospec 3100 pro, Amersham Biosciences, Amersham, England and TrayCell, Hellma GmbH & Co. KG, Müllheim, Germany) for the pure ELP constructs. For all other constructs an absorption measurement at 280 nm led to the concentration (NanoDrop UV-Vis Spectrophotometer, Thermo Fisher Scientific Inc., Waltham, MA, USA). The extinction coefficient was determined theoretically for ELPs at 205 nm[40] and 280 nm[41] for all other fusion proteins.

AFM sample preparation

Force Spectroscopy measurement samples, measurements and data analysis were prepared and performed according to previously published protocols:[10,35] Silicon nitride cantilevers (Biolever mini, BL-AC40TS-C2, Olympus Corporation, Tokyo, Japan; nominal spring constant: 100 pN/nm; 25 kHz resonance frequency in water), were used as force probes. Surface chemistry for cantilevers was similar as for coverslips (Menzel Gläser, Braunschweig, Germany; diameter 24mm). Surfaces were amino silanized with 3-Aminopropyl dimethyl ethoxysilane (APDMES, ABCR GmbH, Karlsruhe, Germany). α-Maleinimidohexanoic-ω-NHS PEG (NHS-PEG-Mal, Rapp Polymere, Tübingen, Germany; PEG-MW: 15 kDa) was used as a linker for the Sortase peptides (GGGGG-C and C-LPETGG, Centic Biotec, Heidelberg, Germany) in PEG linked experiments. The cysteine

containing ELPs were linked to the surface with a sulfosuccinimidyl 4-(N-maleimidomethyl)cyclohexane-1-carboxylate) (sulfo-SMCC, Thermo Fisher Scientific Inc., Waltham, MA, USA). 10 mM of PEG or crosslinker were dissolved in 50 mM 4-(2-hydroxyethyl)-1-piperazineethanesulfonic acid (HEPES) pH 7.5.
Sortase catalyzed coupling of the fingerprint molecules (GGG-CBM-Xmod-DocIII and CohIII-CBM-LPETGG) was done in 25 mM TRIS-HCl, pH 7.2, 5 mM $CaCl_2$, 75 mM NaCl at 22°C for 2 hrs. Typically, 50 µM ELP or Sortase peptide was coupled with 25 µM fingerprint molecule and 2 µM Sortase enzyme.
In between both of the crosslinking steps (PEG, SMCC or ELP, peptide reaction) surfaces were rinsed with water and dried with nitrogen. After immobilization of the fingerprint molecules, surfaces were rinsed in measurement buffer (25 mM TRIS-HCl, pH 7.2, 5 mM $CaCl_2$, 75 mM NaCl). The reaction of the different surface chemistry was done spatially separated by using silicone masks (CultureWell™ Reusable Gaskets, Grace Bio-Labs, Bend, OR, USA). The mask was applied after silanization and removed under buffer after the last immobilization step.

AFM-SMFS measurements

Data was taken on custom built instruments (MFP-3D AFM controller, Oxford Instruments Asylum Research, Inc, Santa Barbara, CA, USA; piezo nanopositioners: Physik Instrumente (PI) GmbH & Co. KG, Karlsruhe, Germany or attocube systems AG, Munich, Germany).
Instrument control software was custom written in Igor Pro 6.3 (Wavemetrics Inc, Portland, OR, USA). Piezo position was controlled with a closed-loop feedback system running internally on the AFM controller field-programmable gate array (FPGA). A typical AFM measurement took about 12 hrs and was done fully automated and at room temperature. Retraction velocity for constant speed force spectroscopy measurements was 0.8 µm/s. Cantilever spring constants were calibrated after completing all measurements on different spots on the surface using the same cantilever. This was done by utilizing the thermal method applying the equipartition theorem to the one dimensionally oscillating lever.[31,42]

Force-extension data analysis

Obtained data were analyzed with custom written software in Python (Python Software Foundation. Python Language Reference, version 2.7. Available at http://www.python.org), utilizing the libraries NumPy and SciPy and Matplotlib.
Raw voltage data traces were transformed into force distance traces with their respective calibration values after determining the zero force value with the baseline position. A correction of the force dependent cantilever tip z-position was carried out. Force distance traces were filtered for traces showing two CBM unfoldings and a subsequent type III Cohesin:Dockerin dissociation, without preceding Xmodule unfolding.[7] This screening was carried out by detecting maximum-to-maximum distances of kernel density estimates (gaussian kernel, bandwidth 1 nm) peaks in contour length space in each single trace, after applying thresholds for force, distance and number of peaks. Remaining traces were excluded from further analysis. For sorting datasets, transformation of force distance data into contour length space was done with an manually fixed persistence length of 0.4 nm, to measure distances of energy barrier positions.[29,43] Sorting was done allowing generous errors to the expected increments to account for the conformational stretching of the spacer molecules. Fits to the force-extension data with the WLC model had following parameters additionally to the values mentioned in the figure captions, if not stated otherwise: initial guess for persistence length: 0.4 nm; fit precision 1e-7. For assessment of transformation

quality, the inverse worm-like-chain model was applied for transformation of force distance traces into the contour length space in a force window of 10 to 125 pN and with a persistence length previously fitted to each peak separately: The global mean value of each dataset for each peak was used. Final alignments of the whole datasets were assembled by cross-correlation.

Master curves assembly

The master curves were assembled by cross-correlation of each force-distance trace of a presorted dataset with all previous curves in contour length space, starting with a random curve. Each curve was shifted on its x axis to fit the maximum correlation value, and added to the set assembly in contour length space. Subsequently, a second run was performed, cross-correlating each curve with the previously assembled set, to facilitate an equal correlation template for every curve, independent of its occurrence. Finally, the most probable shift was calculated by a KDE and subtracted from each curve to get representative absolute distances respective to the origin. Distance and correlation value thresholds were applied to filter out less probable PEG populations and otherwise badly fitting data. In a final step, all overlaid raw data points in force-distance space were binned on the x axis into nanometer sized slices and their densities on the y axis were estimated by a KDE for each slice. Their most probable value and the corresponding full width half maxima then assembled the master curve. By this procedure the most probable and most representative pathway of a dataset was reproduced.

The qmWLC model

For WLC fits and transformations into contour length space, a recently improved approximation, solved for the extension was used[32], adding correction terms for quantum mechanical (qm) backbone stretching.[33]

With the abbreviations

$$f = FL_p/kT \tag{1}$$

$$b = \exp\left(\sqrt[4]{\frac{900}{f}}\right) \tag{2}$$

WLC fits were done with the model formula:

$$x = L_{corr}\frac{4}{3} - \frac{4}{3\sqrt{f+1}} - \frac{10b}{\sqrt{f}(b-1)^2} + \frac{f^{1.62}}{3.55+3.8f^{2.2}} \tag{3}$$

With the quantum mechanical correction:

$$L_{corr} = \frac{L_{c,0}}{2y_2}(\sqrt{4Fy_2+y_1^2} - y_1 + 2y_2) \tag{4}$$

And transformations were performed with model contour length:

$$L_c = \frac{x}{\frac{4}{3} - \frac{4}{3\sqrt{f+1}} - \frac{10b}{\sqrt{f}(b-1)^2} + \frac{f^{1.62}}{3.55+3.8f^{2.2}}} \tag{5}$$

With the reverse quantum mechanical correction for zero force contour length:

$$L_{c,0} = \frac{L_c}{\frac{1}{2y_2}(\sqrt{y_1^2 + 4y_2F} + 2y_2 - y_1)} \quad (6)$$

With x, the extension, L_c the model contour length, F the force, L_p, the persistence length, k the boltzmann's constant, T the temperature, y_1 and y_2 quantum mechanical correction parameters, L_{corr} the qm corrected contour length and $L_{c,0}$ the reverse qm corrected contour length at zero force. As non-linear fitting algorithm, a Levenberg-Marquardt least squares minimization method was applied.

Conflict of interest: The authors declare no competing financial interest.

Supporting Information Available: Further details on experimental methods and supplementary results. This material is available free of charge *via* the Internet at http://pubs.acs.org.

Acknowledgements

This work was supported by the Advanced Grant "Cellufuel" of the European Research Council, the Deutsche Forschungsgemeinschaft through SFB 1032, and from Society in Science - the Branco Weiss Fellowship from ETH Zürich. We thank T. Verdorfer and C. Schoeler for proofreading and helpful discussion.

References

(1) Cao, Y.; Li, H. Engineered Elastomeric Proteins with Dual Elasticity Can Be Controlled by a Molecular Regulator. *Nat. Nanotechnol.* **2008**, *3*, 512–516.
(2) Lv, S.; Dudek, D. M.; Cao, Y.; Balamurali, M. M.; Gosline, J.; Li, H. Designed Biomaterials to Mimic the Mechanical Properties of Muscles. *Nature* **2010**, *465*, 69–73.
(3) Rivas-Pardo, J. A.; Eckels, E. C.; Popa, I.; Kosuri, P.; Linke, W. A.; Fernández, J. M. Work Done by Titin Protein Folding Assists Muscle Contraction. *Cell Reports* **2016**, *14*, 1339–1347.
(4) Ott, W.; Jobst, M. A.; Schoeler, C.; Gaub, H. E.; Nash, M. A. Single-Molecule Force Spectroscopy on Polyproteins and Receptor–ligand Complexes: The Current Toolbox. *J. Struct. Biol.* **2017**, *197*, 3–12.
(5) Bull, M. S.; Sullan, R. M. A.; Li, H.; Perkins, T. T. Improved Single Molecule Force Spectroscopy Using Micromachined Cantilevers. *ACS Nano* **2014**, *8*, 4984–4995.
(6) Stahl, S. W.; Nash, M. A.; Fried, D. B.; Slutzki, M.; Barak, Y.; Bayer, E. A.; Gaub, H. E. Single-Molecule Dissection of the High-Affinity Cohesin-Dockerin Complex. *Proc. Natl. Acad. Sci. U. S. A.* **2012**, *109*, 20431–20436.
(7) Schoeler, C.; Malinowska, K. H.; Bernardi, R. C.; Milles, L. F.; Jobst, M. A.; Durner, E.; Ott, W.; Fried, D. B.; Bayer, E. A.; Schulten, K.; E, G. H.; Nash, M. A. Ultrastable Cellulosome-Adhesion Complex Tightens under Load. *Nat. Commun.* **2014**, *5*, 1–8.
(8) Baumann, F.; Bauer, M. S.; Milles, L. F.; Alexandrovich, A.; Gaub, H. E.; Pippig, D. A. Monovalent Strep-Tactin for Strong and Site-Specific Tethering in Nanospectroscopy. *Nat. Nanotechnol.* **2015**, *11*, 89–94.
(9) Milles, L. F.; Bayer, E. A.; Nash, M. A.; Gaub, H. E. Mechanical Stability of a High-Affinity Toxin Anchor from the Pathogen Clostridium Perfringens. *J. Phys. Chem. B*

2017, *121*, 3620–3625.
(10) Zimmermann, J. L.; Nicolaus, T.; Neuert, G.; Blank, K. Thiol-Based, Site-Specific and Covalent Immobilization of Biomolecules for Single-Molecule Experiments. *Nat. Protoc.* **2010**, *5*, 975–985.
(11) Zakeri, B.; Fierer, J. O.; Celik, E.; Chittock, E. C.; Schwarz-Linek, U.; Moy, V. T.; Howarth, M. Peptide Tag Forming a Rapid Covalent Bond to a Protein, through Engineering a Bacterial Adhesin. *Proc. Natl. Acad. Sci. U. S. A.* **2012**, *109*, E690–E697.
(12) Popa, I.; Rivas-Pardo, J. A.; Eckels, E. C.; Echelman, D.; Valle-Orero, J.; Fernandez, J. M. A HaloTag Anchored Ruler for Week-Long Studies of Protein Dynamics. *J. Am. Chem. Soc.* **2016**, *138*, 10546–10553.
(13) Popa, I.; Berkovich, R.; Alegre-Cebollada, J.; Badilla, C. L.; Rivas-Pardo, J. A.; Taniguchi, Y.; Kawakami, M.; Fernandez, J. M. Nanomechanics of HaloTag Tethers. *J. Am. Chem. Soc.* **2013**, *135*, 12762–12771.
(14) Pippig, D. A.; Baumann, F.; Strackharn, M.; Aschenbrenner, D.; Gaub, H. E. Protein-DNA Chimeras for Nano Assembly. *ACS Nano* **2014**, *8*, 6551–6555.
(15) Otten, M.; Ott, W.; Jobst, M. A.; Milles, L. F.; Verdorfer, T.; Pippig, D. A.; Nash, M. A.; Gaub, H. E. From Genes to Protein Mechanics on a Chip. *Nat. Methods* **2014**, *11*, 1127–1130.
(16) Oesterhelt, F.; Rief, M.; Gaub, H. E. Single Molecule Force Spectroscopy by AFM Indicates Helical Structure of Poly(ethylene-Glycol) in Water. *New J. Phys.* **1999**, *1*, 1–11.
(17) Liese, S.; Gensler, M.; Krysiak, S.; Schwarzl, R.; Achazi, A.; Paulus, B.; Hugel, T.; Rabe, J. P.; Netz, R. R. Hydration Effects Turn a Highly Stretched Polymer from an Entropic into an Energetic Spring. *ACS Nano* **2017**, *11*, 702–712.
(18) Xue, Y.; Li, X.; Li, H.; Zhang, W. Quantifying Thiol-Gold Interactions towards the Efficient Strength Control. *Nat. Commun.* **2014**, *5*, 4348.
(19) Ott, W.; Nicolaus, T.; Gaub, H. E.; Nash, M. A. Sequence-Independent Cloning and Post-Translational Modification of Repetitive Protein Polymers through Sortase and Sfp-Mediated Enzymatic Ligation. *Biomacromolecules* **2016**, *17*, 1330−1338.
(20) Tang, N. C.; Chilkoti, A. Combinatorial Codon Scrambling Enables Scalable Gene Synthesis and Amplification of Repetitive Proteins. *Nat. Mater.* **2016**, *15*, 419–424.
(21) McDaniel, J. R.; MacKay, J. A.; Quiroz, F. G.; Chilkoti, A. Recursive Directional Ligation by Plasmid Reconstruction Allows Rapid and Seamless Cloning of Oligomeric Genes. *Biomacromolecules* **2010**, *11*, 944–952.
(22) Meyer, D. E.; Chilkoti, A. Genetically Encoded Synthesis of Protein-Based Polymers with Precisely Specified Molecular Weight and Sequence by Recursive Directional Ligation: Examples from the Elastin-like Polypeptide System. *Biomacromolecules* **2002**, *3*, 357–367.
(23) Gray, W. R.; Sandberg, L. B.; Foster, J. A. Molecular Model for Elastin Structure and Function. *Nature* **1973**, *246*, 461–466.
(24) Roberts, S.; Dzuricky, M.; Chilkoti, A. Elastin-like Polypeptides as Models of Intrinsically Disordered Proteins. *FEBS Lett.* **2015**, *589*, 2477–2486.
(25) Dorr, B. M.; Ham, H. O.; An, C.; Chaikof, E. L.; Liu, D. R. Reprogramming the Specificity of Sortase Enzymes. *Proc. Natl. Acad. Sci. U. S. A.* **2014**, *111*, 13343–13348.
(26) Urry, D. W.; Hugel, T.; Seitz, M.; Gaub, H. E.; Sheiba, L.; Dea, J.; Xu, J.; Parker, T. Elastin: A Representative Ideal Protein Elastomer. *Philos. Trans. R. Soc., B* **2002**, *357*, 169–184.
(27) Valiaev, A.; Lim, D. W.; Oas, T. G.; Chilkoti, A.; Zauscher, S. Force-Induced Prolyl Cis-Trans Isomerization in Elastin-like Polypeptides. *J. Am. Chem. Soc.* **2007**, *129*, 6491–6497.
(28) Valiaev, A.; Dong, W. L.; Schmidler, S.; Clark, R. L.; Chilkoti, A.; Zauscher, S. SI: Hydration and Conformational Mechanics of Single, End-Tethered Elastin-like Polypeptides. *J. Am. Chem. Soc.* **2008**, *130*, 10939–10946.
(29) Puchner, E. M.; Franzen, G.; Gautel, M.; Gaub, H. E. Comparing Proteins by Their Unfolding Pattern. *Biophys. J.* **2008**, *95*, 426–434.

(30) Dietz, H.; Rief, M. Exploring the Energy Landscape of GFP by Single-Molecule Mechanical Experiments. *Proc. Natl. Acad. Sci. U. S. A.* **2004**, *101*, 16192–16197.
(31) Proksch, R.; Schäffer, T. E.; Cleveland, J. P.; Callahan, R. C.; Viani, M. B. Finite Optical Spot Size and Position Corrections in Thermal Spring Constant Calibration. *Nanotechnology* **2004**, *15*, 1344–1350.
(32) Petrosyan, R. Improved Approximations for Some Polymer Extension Models. *Rheol. Acta* **2017**, *56*, 21–26.
(33) Hugel, T.; Rief, M.; Seitz, M.; Gaub, H. E.; Netz, R. R. Highly Stretched Single Polymers: Atomic-Force-Microscope Experiments versus Ab-Initio Theory. *Phys. Rev. Lett.* **2005**, *94*, 048301.
(34) Valiaev, A.; Lim, D. W.; Schmidler, S.; Clark, R. L.; Chilkoti, A.; Zauscher, S. Hydration and Conformational Mechanics of Single, End-Tethered Elastin-like Polypeptides. *J. Am. Chem. Soc.* **2008**, *130*, 10939–10946.
(35) Jobst, M. A.; Schoeler, C.; Malinowska, K.; Nash, M. A. Investigating Receptor-Ligand Systems of the Cellulosome with AFM-Based Single-Molecule Force Spectroscopy. *J. Visualized Exp.* **2013**, e50950.
(36) Stirnemann, G.; Giganti, D.; Fernandez, J. M.; Berne, B. J. Elasticity, Structure, and Relaxation of Extended Proteins under Force. *Proc. Natl. Acad. Sci. U. S. A.* **2013**, *110*, 3847–3852.
(37) Cheng, S.; Cetinkaya, M.; Gräter, F. How Sequence Determines Elasticity of Disordered Proteins. *Biophys. J.* **2010**, *99*, 3863–3869.
(38) Studier, F. W. Protein Production by Auto-Induction in High Density Shaking Cultures. *Protein Expression Purif.* **2005**, *41*, 207–234.
(39) MacEwan, S. R.; Hassouneh, W.; Chilkoti, A. Non-Chromatographic Purification of Recombinant Elastin-like Polypeptides and Their Fusions with Peptides and Proteins from Escherichia Coli. *J. Visualized Exp.* **2014**, e51583.
(40) Anthis, N. J.; Clore, G. M. Sequence-Specific Determination of Protein and Peptide Concentrations by Absorbance at 205 Nm. *Protein Sci.* **2013**, *22*, 851–858.
(41) Gasteiger, E.; Hoogland, C.; Gattiker, A.; Duvaud, S.; Wilkins, M.; Appel, R.; Bairoch, A. Protein Identification and Analysis Tools on the ExPASy Server. *The Proteomics Protocols Handbook* **2005**, 571–607.
(42) Hutter, J. L.; Bechhoefer, J. Calibration of Atomic-Force Microscope Tips. *Rev. Sci. Instrum.* **1993**, *64*, 1868–1873.
(43) Jobst, M. A.; Milles, L. F.; Schoeler, C.; Ott, W.; Fried, D. B.; Edward, A.; Gaub, H. E.; Nash, M. A. Resolving Dual Binding Conformations of Cellulosome Cohesin- Dockerin Complexes Using Single-Molecule Force Spectroscopy. *eLife* **2015**.

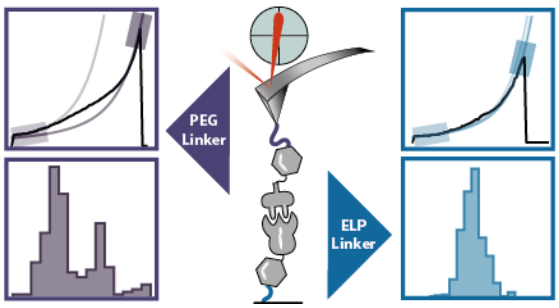

Table of Content Graphic

Supporting Information:
Elastin-Like Polypeptide Linkers for Single Molecule Force Spectroscopy

Wolfgang Ott[a,b,⊥], Markus A. Jobst[a, ⊥], Magnus S. Bauer[a], Ellis Durner[a], Lukas F. Milles[a], Michael A. Nash[c,d], Hermann E. Gaub[a,#]

[a] Lehrstuhl für Angewandte Physik and Center for NanoScience, Ludwig-Maximilians-Universität, 80799 Munich, Germany.

[b] Center for Integrated Protein Science Munich (CIPSM), Ludwig-Maximilians-Universität, 81377 Munich, Germany.

[c] Department of Chemistry, University of Basel, 4056 Basel, Switzerland.

[d] Department of Biosystems Science and Engineering, Swiss Federal Institute of Technology (ETH Zurich), 4058 Basel, Switzerland.

[⊥] These authors contributed equally to this work

[#] Corresponding author: gaub@lmu.de

Supporting Information

Cloning of ELP linkers. Standard PCR was used for amplification of DNA (Phusion High-Fidelity PCR Master Mix, Thermo Fisher Scientific Inc., Waltham, MA, USA). Melting temperatures were adjusted according to the employed primers (see Table S1, below).

A plasmid encoding ybbR-ELP$_{120nm}$-LPETGG described earlier by Ott *et al.*[1] was modified to yield the plasmid Cys-ELP$_{120nm}$-LPETGG. PCR amplification of the plasmid with primers annealing at and downstream of the ybbR-tag was the first step (**Supplemental Figure S1**). The gene for the ELP is a highly repetitive sequence, hence it was necessary to anneal the forward primer at the ybbR-tag to create a unique attachment site. Since the ybbR-tag had to be removed, a *Bsa*I restriction site was incorporated with a primer downstream of the annealing region of the forward primer. The reverse primer had a cysteine encoded at its 5' end. After successful PCR amplification, the product was digested (*Bsa*I and *Dpn*I) and blunted (1h, 37°C, 5 Min, 80°C). The blunting reaction was performed in parallel with 1 µl of Klenow Fragment enzyme and the addition of 1 mM dNTPs (Thermo Fisher Scientific Inc., Waltham, MA, USA)).
After purification (QIAquick PCR purification kit or gel extraction kit (Qiagen GmbH, Hilden, Germany) the ligation reaction was set up: 1 µl of a T4 Ligase (10U/µl, Thermo Fisher Scientific Inc., Waltham, MA, USA was supplemented with 1 µl ATP (10 mM), 0.5 µl PEG-6000, 1 µl T4 Polynucleotide Kinase (PNK) and buffered in CutSmart buffer (New England Biolabs, Ipswich, MA, USA).

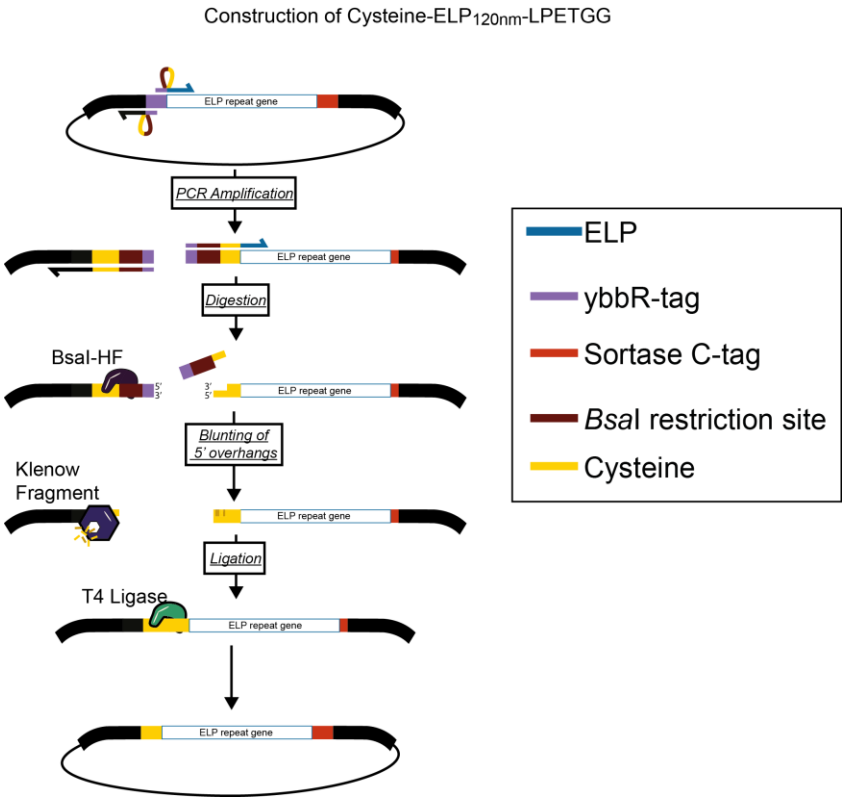

Supplemental Figure S1. Cloning scheme for Cys-ELP$_{120nm}$-LPETGG.

For the creation of the TEV-GGG-ELP$_{60nm}$-LPETGG plasmid, a plasmid encoding ybbR-ELP$_{60nm}$-LPETGG[1] was mutated with one QuikChange primer[2], annealing up- and downstream of the ybbR-tag introducing DNA encoding a TEV-site and a triple glycine. The TEV cleavage site was introduced to ensure full cleavage of the N-terminal methionine. This was assumed to be necessary, since Sortase A only works with glycines at the very N-terminal start of a protein. The QuikChange reaction was done with 50 ng DNA template, 1 µl of primer (10 pmol/µl) in 20 µl Phusion High-Fidelity PCR Master Mix (Thermo Fisher Scientific Inc., Waltham, MA, USA, see **Supplemental Figure S2**).

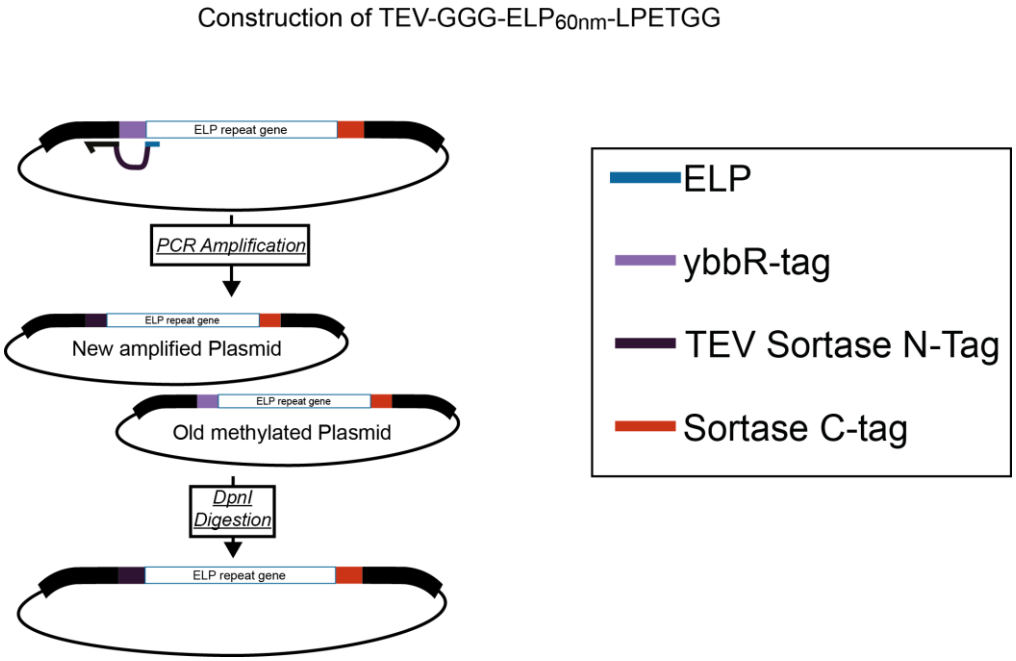

Supplemental Figure S2. Cloning scheme for TEV-GGG-ELP$_{60nm}$-LPETGG.

The newly obtained plasmid was modified again with QuikChange to exchange the C-terminal Sortase-tag with a ybbR-tag (**Supplemental Figure S3**).

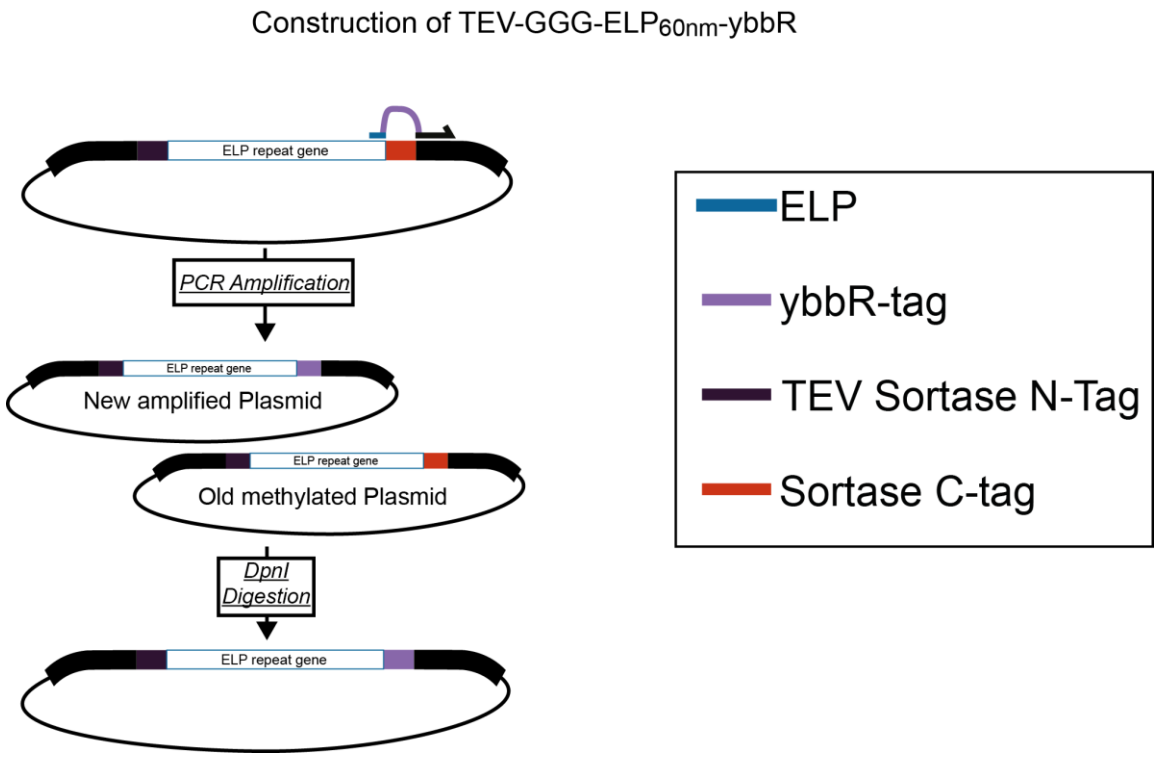

Supplemental Figure S3. Cloning scheme for TEV-GGG-ELP$_{60nm}$-ybbR.

The ELP gene cassette was duplicated by insertion of a gene sequence encoding [$(VPGVG)_5$-$(VPGAG)_2$-$(VPGGG)_3$]$_3$ into the linearized vector containing TEV-GGG-ELP_{60nm}-ybbR. This was done by GoldenGate cloning.[3] For this purpose, both vector and insert were amplified with primers encoding flanking *Bsa*I restriction sites. The *Bsa*I sites were designed to match the corresponding end of insert and backbone, without leaving any cloning scars. After *Bsa*I digestion and purification of the PCR product *via* gel extraction, both of the parts were ligated with their corresponding sticky ends (2.5 µl CutSmart buffer, 1.25 µl T7 ligase, 2.5 µl ATP (10 mM); New England Biolabs, Ipswich, MA, USA, see **Supplemental Figure S4**).

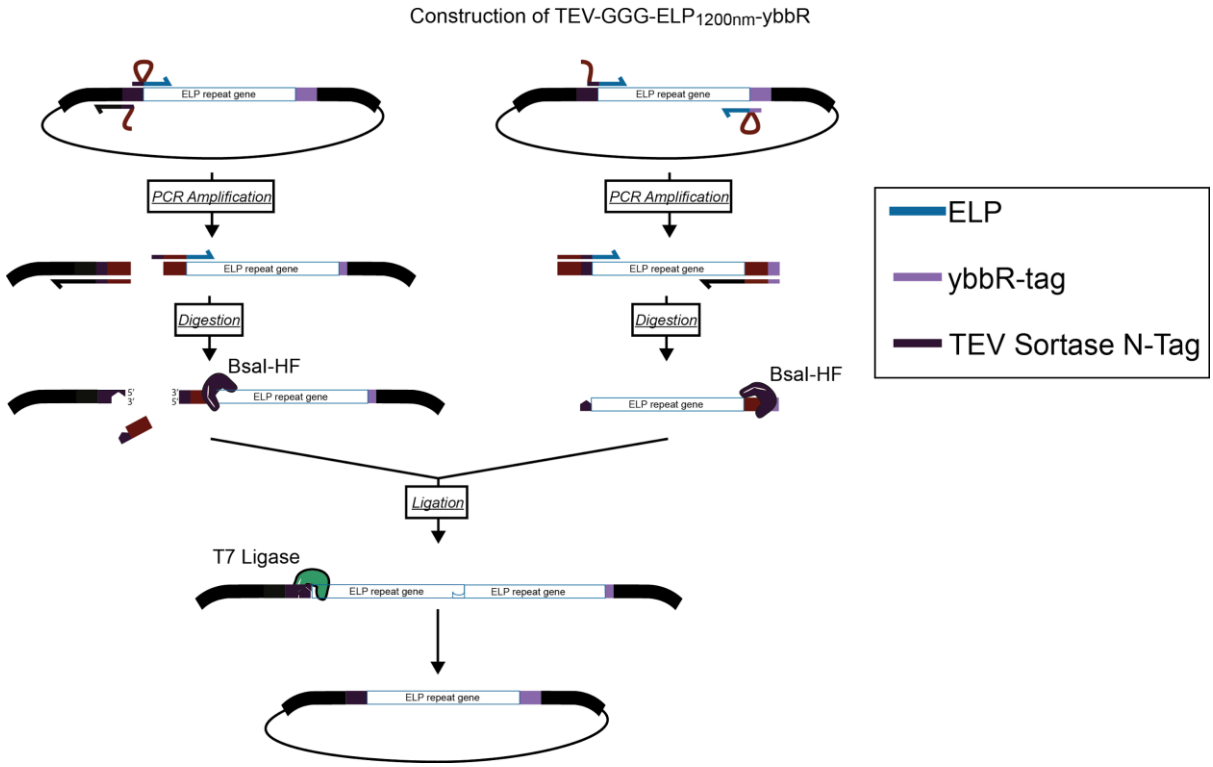

Supplemental Figure S4. Cloning scheme for TEV-GGG-ELP_{120nm}-ybbR.

Experiments showed that the *E. coli* methionine aminopeptidases already fully digested the N-terminal methionine proceeding the polyglycine. Hence, removal of the TEV cleavage site was desired to simplify the ELP production process. This was achieved by a linearization reaction, *Bsa*I digestion and religation as described above. Primers were designed to anneal at the TEV-site and encoded a *Bsa*I restriction site upstream of the triple glycine (**Supplemental Figure S5**).

Construction of GGG-ELP$_{120nm}$-ybbR

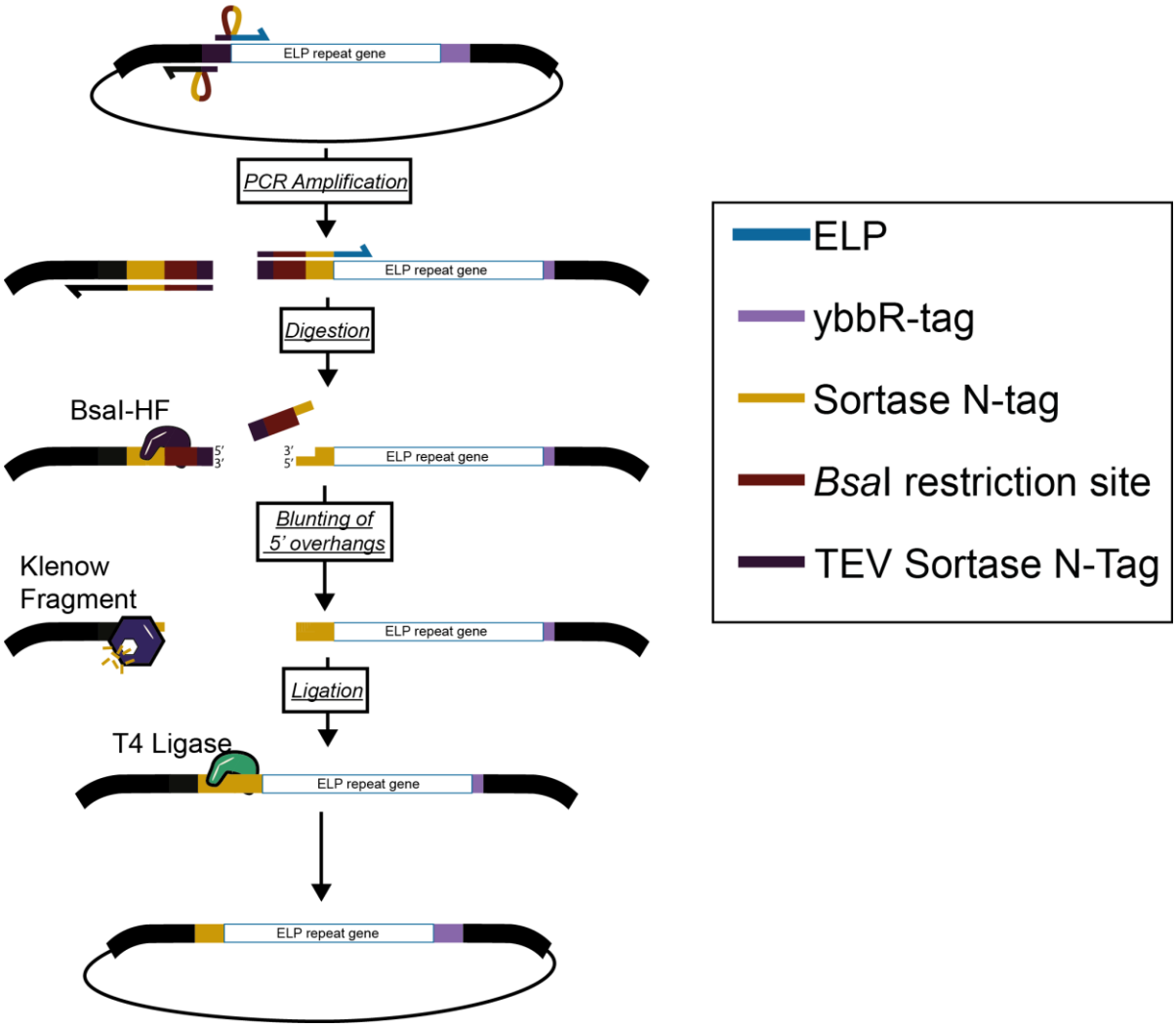

Supplemental Figure S5. Cloning scheme for GGG-ELP$_{120nm}$-ybbR

Finally, the C-terminal ybbR-tag was switched to a cysteine. The reverse primer attached at the codons of the ybbR-tag with a *Bsa*I restriction site. The forward primer encoded a cysteine at its 5' end and annealed downstream of the stop codon. The linear plasmid was processed as described above (**Supplemental Figure S6**).

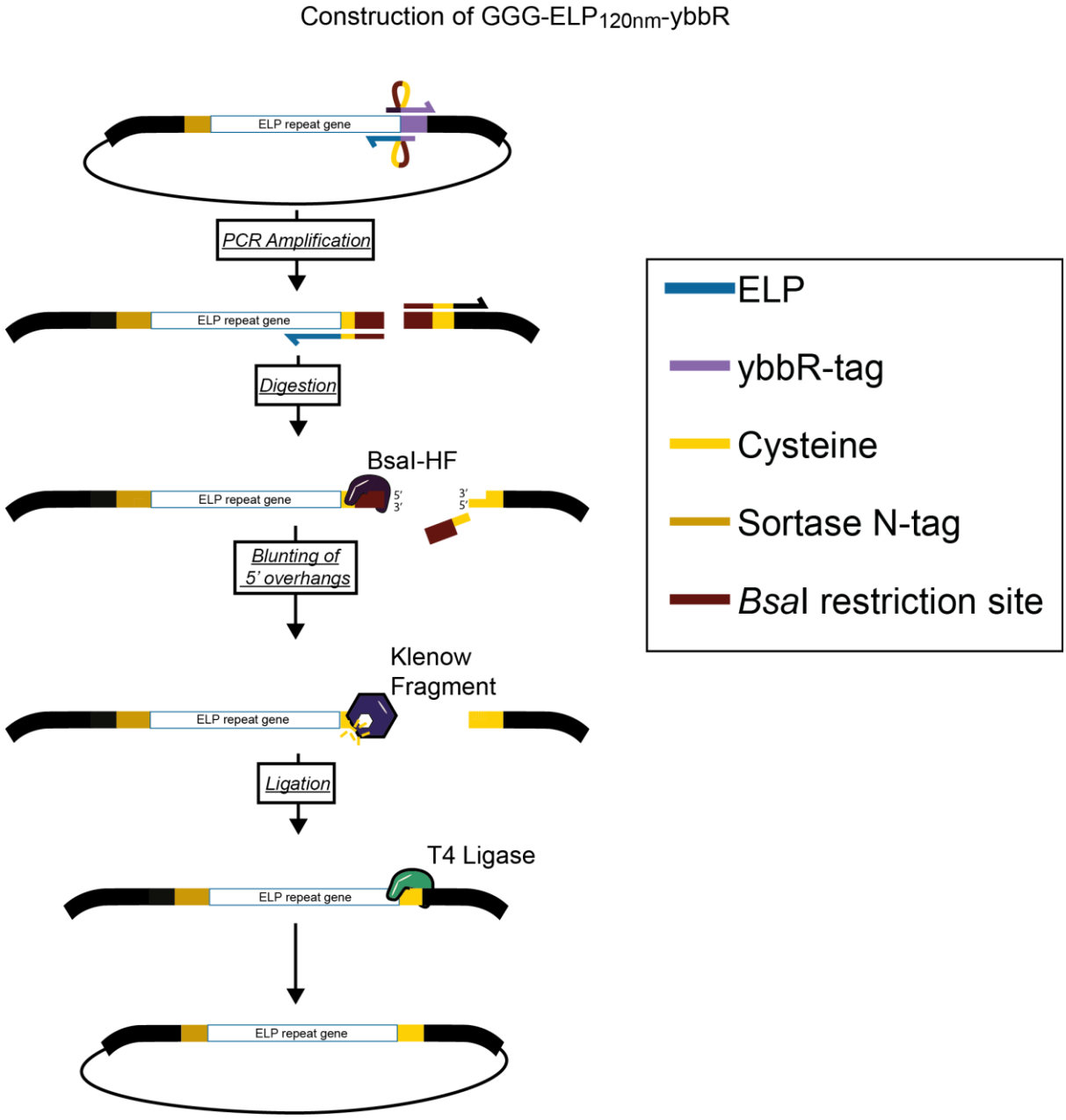

Supplemental Figure S6. Cloning scheme for GGG-ELP$_{120nm}$-Cys

Cloning of GGG-HIS-CBM-Xmod-DocIII and CohIII-CBM-HIS-LPETGG.
Basis for the construction were two plasmids published by Schoeler *et al.*[4] The plasmid encoding the gene for CohIII-CBM was linearized with primers encoding the Sortase C-tag. 4.5 µl of the PCR product was directly digested with 1 µl *Dpn*I (Thermo Fisher Scientific Inc., Waltham, MA, USA), 3' ends were phosphorylated with 1 µl T4 PNK (New England Biolabs, Ipswich, MA, USA) and the ends were religated with 1 µl T4 Ligase (10U/µl, Thermo Fisher Scientific Inc., Waltham, MA, USA) (15 Min at 37°C, 45 Min 22°C). The 10 µl reaction was supplemented with 1 µl ATP (10 mM), 0.5 µl PEG-6000 and 1 µl CutSmart buffer (10x, New England Biolabs, Ipswich, MA, USA).

The plasmid encoding the CohIII domain had a cloning scar with the amino acids "MGT" at the N-terminus, the glycine and threonine were removed since one single glycine is already reactive with the "LPETGG" in a Sortase A catalyzed reaction. This was done with a sequential linearization and religation reaction (as described above).

The CBM-Xmod-DocIII gene was subcloned with Gibson Assembly into a linearized vector with a TEV site followed by a Sortase N-tag. 10 µl of the HiFi MasterMix (2x, New England Biolabs, Ipswich, MA, USA), were mixed with a 10-fold molar excess of insert to the backbone (reaction volume 20 µl, 1 hr, 50°C; **Supplemental Figure S7**). Similar to the GGG-ELP$_{120nm}$-Cys, the unnecessary TEV site was removed, since *E. coli* already digested the N-terminal methionine sufficiently. This was achieved by employing the same procedure as described for CohIII-CBM linearization and religation.

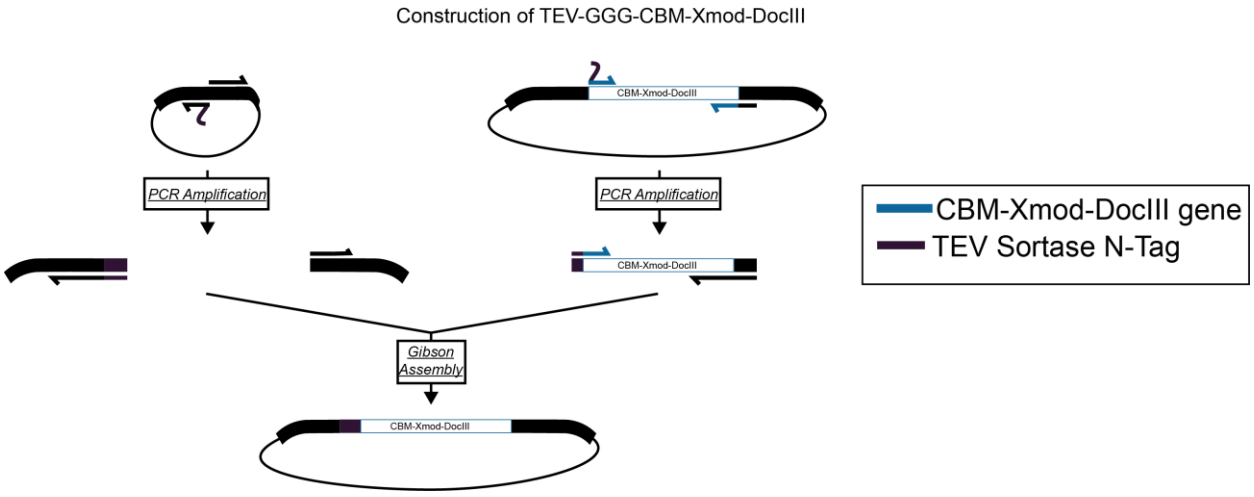

Supplemental Figure S7. Cloning scheme for TEV-GGG-CBM-Xmod-DocIII

Supplemental Table S1. Overview of primers

Name	**Sequence (5'-3')**
Construction of Cys-ELP$_{120nm}$-LPETGG	
FW N-Cys BsaI	GACTCTCTGGAATTCATCGCTTCTAAACTGGC TGGTCTCCTGCGTGCCGGGAGAAGGAG
REV BsaI ybbR	CCCGGCACAGCCAGTTTAGAAGCGATGAATTC CAGAGAGTCGGTCTCACATATGTATATC
Construction of TEV-GGG-ELP$_{60nm}$-LPETGG	
QuikChange Primer ybbR to TEV-GGG	GACACCAGGGACTCCTTCTCCCGGCACACCG CCCCCTCCCTGGAAGTACAGGTTTTCCATATG TATATCTCCTTC
Construction of TEV-GGG-ELP$_{60nm}$-ybbR	
QuikChange Primer LPETGG to ybbR	GACACCAGGGACTCCTTCTCCCGGCACACCG CCCCCTCCCTGGAAGTACAGGTTTTCCATATG TATATCTCCTTC
Construction of TEV-GGG-ELP$_{120nm}$-ybbR	
FW backbone BsaI	GAAAACCTGTACTTCCAGGGAGGGGGGTCTC GGGGTGTGCCGGGAGAAGGAG
REV backbone BsaI	ATATATGGTCTCGACCGCCCCCTCCCTGGAAG TACAGGTTTTC
FW insert TEV-GGG BsaI	CCAGGGAGGGGGGTCTCGCGGTGTGCCGGG AGAAGGAG
REV insert BsaI	TCGAGTTAAGCCAGTTTAGAAGCGATGAATTC CAGAGAGTCGGTCTCCACCCTCACCCGG
Construction of GGG-ELP$_{120nm}$-ybbR	
FW ELP GGG	GGGGGCGGTGTGCCGGGAG
REV BsaI TEV	GGCACACCGCCCCCTCCCTGGAAGTACAGGT TTTCGGTCTCACATATGTATATCTCCTTC

Construction of GGG-ELP$_{120nm}$-Cys	
FW backbone Cys	GCCAGTTTAGAAGCGATGAATTCCAGAGAGTC GGTCTCCACCTTCACCC
REV ybbR BsaI	TGCTAACTCGAGTAAGATCCGGCTGCTAACAA AGCCC
Construction of GT-CohIII (R.f)-CBM-HIS-LPETGG	
FW backbone	TAACTCGAGTAAGATCCGGCTGC
REV CBM LPETGG	GCCGCCGGTTTCCGGCAGCGGACCCTGGAAC AGAAC
Construction of CohIII (R.f)-CBM-HIS-LPETGG	
FW CohIII	GCGCTCACAGACAGAGGAATG
REV backbone without GT	CATATGTATATCTCCTTCTTAAAGTTAA
Construction of TEV-GGG-HIS-CBM-XDocIII (R.f.)	
FW backbone	CTCGAGTAAGATCCGGCTGC
REV backbone	ACCGGGTTCTTTACCCC
FW insert	GTATGGGGTAAAGAACCCGGTGGCAGTGTAG TACCATC
REV insert	CGGATCTTACTCGAGTTATTCTTCTTCAGCATC GCCTG
Construction of GGG-HIS-CBM-XDocIII (R.f.)	
FW CBM	ATGGCCAATACACCGGTATCA
REV backbone	TCCGTGGTGGTGGTGGTGGTGACCGCCCCCC ATATGTATATCTC

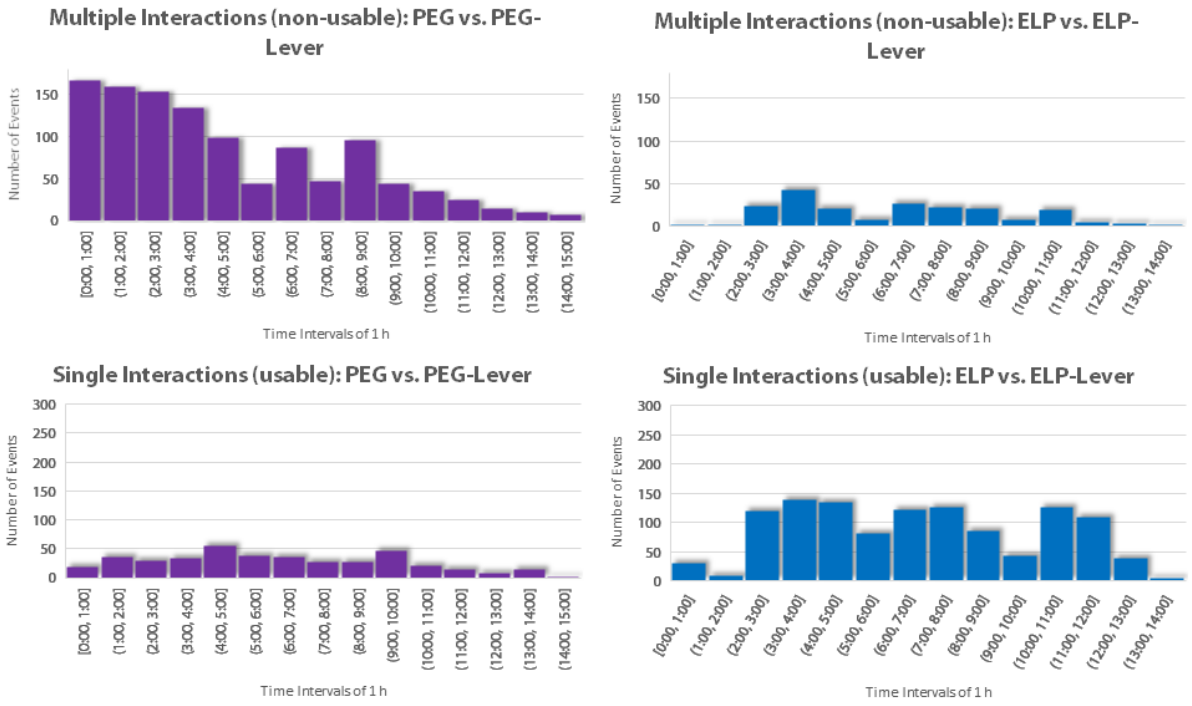

Supplemental Figure S8. Number of curves within a 1 hr timeframe were binned in one histogram bar. Multiple traces were traces with more than 10 peaks (Supplemental Figure S9 shows an exemplary multiple interaction trace). Left (purple) is the PEG-lever versus the PEG-immobilization and right (blue) ELP-lever versus ELP-immobilization. The two top panels show number of multiple interactions over time. The bottom panels show number of single specific interactions over time.

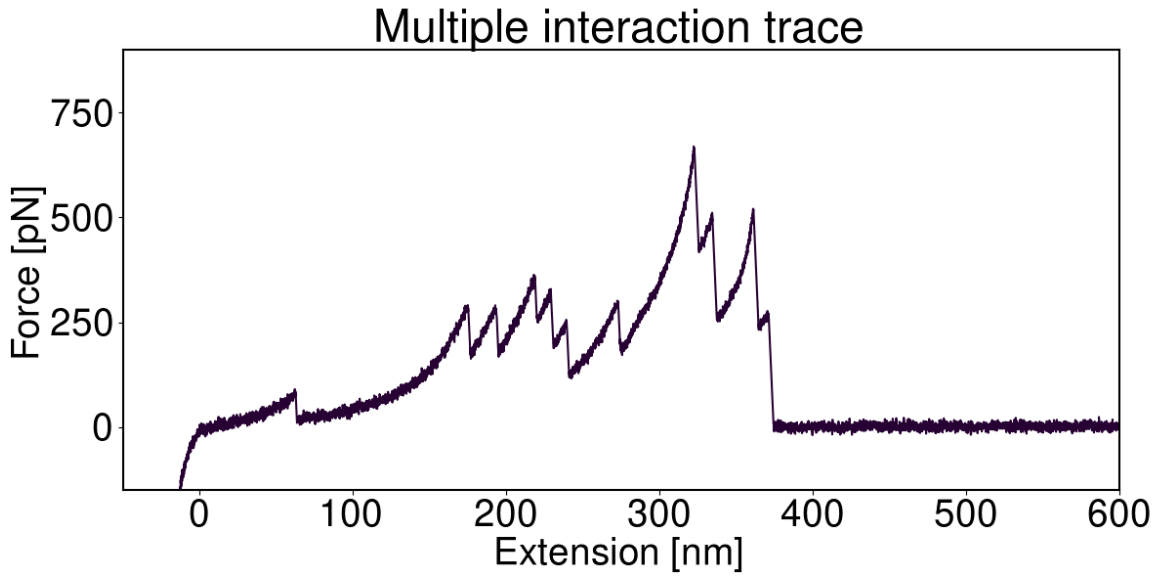

Supplemental Figure S9. A typical example trace displaying multiple interactions.

Supplemental Table S2. Biophysical parameters of the employed ELPs.

ELP repeats $(5)_x$	ε_{205} [1/M cm][5]	Molecular weight [Da][6]	Isoelectric point	Amino acids in ELP repeats (total)[6]	Total Length [nm][7] (.365 nm per aa)
Cys-ELP_{60}-LPETGG	851370	24763.08	3.20	300 (307)	112.06
GGG-ELP_{60}-Cys	843030	24379.63	3.23	300 (304)	110.96

Protein Sequences

GGG-ELP_{60}-Cys

Sortase N-Tag
ELP
Cysteine

GGGVPGEGVPGVGVPGVGVPGVGVPGVGVPGAGVPGAGVPGGGVPGGGVPGEGVPGEGV
PGVGVPGVGVPGVGVPGVGVPGAGVPGAGVPGGGVPGGGVPGEGVPGEGVPGVGVPGVG
VPGVGVPGVGVPGAGVPGAGVPGGGVPGGGVPGEGVPGEGVPGVGVPGVGVPGVGVPGV
GVPGAGVPGAGVPGGGVPGGGVPGEGVPGEGVPGVGVPGVGVPGVGVPGVGVPGAGVPG
AGVPGGGVPGGGVPGEGVPGEGVPGVGVPGVGVPGVGVPGVGVPGAGVPGAGVPGGGVP
GGGVPGEGC

Cys-ELP_{60}-LPETGG
Cysteine
ELP
Sortase C-Tag

MCVPGEGVPGVGVPGVGVPGVGVPGVGVPGAGVPGAGVPGGGVPGGGVPGEGVPGEGVP
GVGVPGVGVPGVGVPGVGVPGAGVPGAGVPGGGVPGGGVPGEGVPGEGVPGVGVPGVGV
PGVGVPGVGVPGAGVPGAGVPGGGVPGGGVPGEGVPGEGVPGVGVPGVGVPGVGVPGVG
VPGAGVPGAGVPGGGVPGGGVPGEGVPGEGVPGVGVPGVGVPGVGVPGVGVPGAGVPGA
GVPGGGVPGGGVPGEGVPGEGVPGVGVPGVGVPGVGVPGVGVPGAGVPGAGVPGGGVPG
GGVPGEGLPETGG

MGGG-HIS-CBM-Xmod-Dockerin III (*R. f.*)
Sortase N-Tag
His_6-Tag
CBM
Linker
Xmod
Dockerin III

MGGGHHHHHHGMANTPVSGNLKVEFYNSNPSDTTNSINPQFKVTNTGSSAIDLSKLTLRYYYT
VDGQKDQTFWSDHAAIIGSNGSYNGITSNVKGTFVKMSSSTNNADTYLEISFTGGTLE
PGAHVQIQGRFAKNDWSNYTQSNDYSFKSASQFVEWDQVTAYLNGVLVWGKEPGGSVVPST
QPVTTPPATTKPPATTIPPSDDPNAVVPNTVTSAVKTQYVEIESVDGFYFNTEDKFDTA
QIKKAVLHTVYNEGYTGDDGVAVVLREYESEPVDITAELTFGDATPANTYKAVENKFDYE
IPVYYNNATLKDAEGNDATVTVYIGLKGDTDLNNIVDGRDATATLTYYAATSTDGKDATT
VALSPSTLVGGNPESVYDDFSAFLSDVKVDAGKELTRFAKKAERLIDGRDASSILTFYTK
SSVDQYKDMAANEPNKLWDIVTGDAEEE

Cohesin III (*R.f.*)-CBM-HIS-LPETGG
Cohesin III
Linker
CBM
His_6-Tag
Sortase C-Tag

MALTDRGMTYDLDPKDGSSAATKPVLEVTKKVFDTAADAAGQTVTVEFKVSGAEGKYATT
GYHIYWDERLEVVATKTGAYAKKGAALEDSSLAKAENNGNGVFVASGADDDFGADGVMWTV
ELKVPADAKAGDVYPIDVAYQWDPSKGDLFTDNKDSAQGKLMQAYFFTQGIKSSSNPSTDEYL
VKANATYADGYIAIKAGEPGSVVPSTQPVTTPPATTKPPATTIPPSDDPNAMANTPVSGNLKVE
FYNSNPSDTTNSINPQFKVTNTGSSAIDLSKLTLRYYYTVDGQKDQTFWSDHAAIIGSNGSYNGI
TSNVKGTFVKMSSSTNNADTYLEISFTGGTLEPGAHVQIQGRFAKND
WSNYTQSNDYSFKSASQFVEWDQVTAYLNGVLVWGKEPGELKLPRSRHHHHHHGSLEVLFQ
GPLPETGG

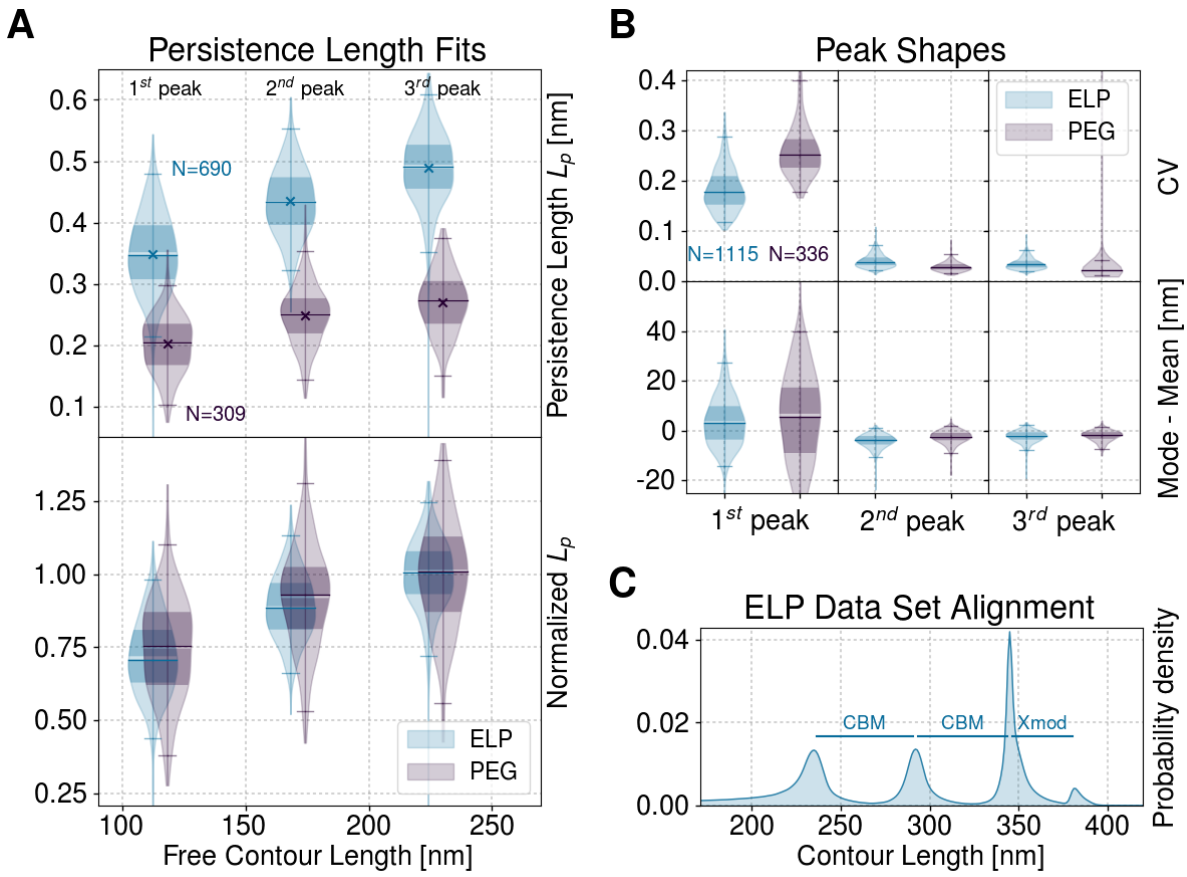

Supplemental Figure S10: Performance of contour length transformations. (A) Observed persistence lengths. Upper plot: observed persistence lengths preceding each CBM and Coh:DocIII unfolding/rupture peak as measured by WLC fits in the force range of 30 to 125 pN (ELP: 0.35, 0.44, and 0.49 nm; PEG: 0.20, 0.25, and 0.27 nm). Lower plot: same data normalized to the respective last peak means. The qualitative behavior over the unfolding of the peaks is similar for both constructs. **(B)** Assessment of transformation quality. Coefficient of variation (CV) as a measure of distribution broadness and distance of mode to mean as a measure of peak symmetry show better performance for ELP data for the first peaks. Later peaks show better performance of PEG data, although the differences are negligible. Transformations were done with the inverse WLC model only for data points between 10 and 125 pN. Persistence lengths for the transformations were chosen as the mean values of the WLC fits to each peak as shown in panel (A). **(C)** Alignment of transformed ELP curves in contour length space. Two CBM increments and one Xmod unfolding prior to Coh:Doc rupture are clearly detectable.

Low force performance of ELP linkers

For this analysis, only forces in a range from 10 to 125 pN were taken into account, to minimize the effects of conformational stretching. The elastic properties of the first stretching event of a data trace are dominated by the linker molecules. As more protein domains unfold, the peptide backbone of the unfolded domains contributes increasingly to the overall elastic response. Contour length transformations of force distance data (data not shown) were performed with the mean fitted persistence lengths of each peak, as shown in **Supplemental Figure S10, Panel A** (0.35, 0.44, and 0.49 nm for ELP data peaks; 0.20, 0.25, and 0.27 nm for PEG data peaks), to

account for varying persistence lengths over the course of each pulling cycle. The persistence length as a measure for the stiffness of a polymer is lower for PEG than for ELP with bulky side chains and rotational restrictions of the peptide backbone. Comparable changes of persistence lengths over the course of an unfolding experiment were also observed earlier in other studies.[8,9] The distribution width and asymmetry of each peak in contour length space were evaluated separately by the coefficient of variation and the calculated difference of statistical mode and mean. A comparison of all datasets revealed that for the first unfolding peak, ELP datasets display slightly superior properties: the first peak for data with ELP linker tethering is sharper and more symmetric (**Supplemental Figure S10, Panel B**) as indicated by the narrower distribution and lower coefficient of variation. For the subsequent peaks 2 and 3, both PEG and ELP linkers perform similarly and the differences become negligibly small. Although the impact on data quality in this low force regime examined here, was not as severe as expected, ELP linkers seem to exhibit advantageous behavior for the first stretching events of each curve, and might improve accuracy in determining the following contour length increments to identify protein domains.

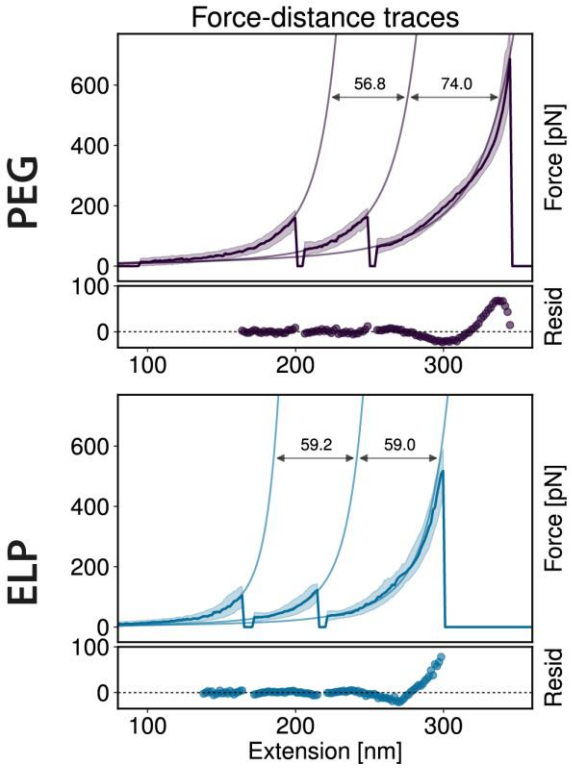

Supplemental Figure S11: Master curves fits with persistence lengths as an additional free fit parameter. If the persistence length is not kept fix, but also fitted to the data, it is clearly visible, that this parameter is optimized to compensate the conformational stretching effect for PEG datasets. While the qmWLC model fit itself looks better and has lower residuals compared to the fixed persistence length fit, the resulting contour length increment is way off and does not yield any meaningful value, rendering the model useless to extract information from the data. The two CBM domains have the exact same amino acid sequence and therefore should show the same contour length increments upon unfolding.

Linker Length. The artefacts generated by PEG linkers at elevated forces might be reduced by shortening the linker molecules. Usually our force spectroscopy experiments employ spacers with 40 nm length. Many SMFS assays utilize these 5 kDa PEG linkers, where the effect is scaled down proportionally with length, however still present. Further truncation would minimize the influence of the conformational change of PEG spacers, but in return raise other concerns: i) reduced mechanical isolation of the molecules under investigation by low pass filtering from transducer oscillations, to ensure purely thermally driven unfolding and dissociation events[10], ii) reduced passivation of the surfaces against nonspecific adsorption, and iii) influence of surface effects and effects of the linker molecules themselves on the domains of interest. Employing peptide based smart polymers as linkers offer a new solution to this issue, avoiding linker artefacts almost entirely.

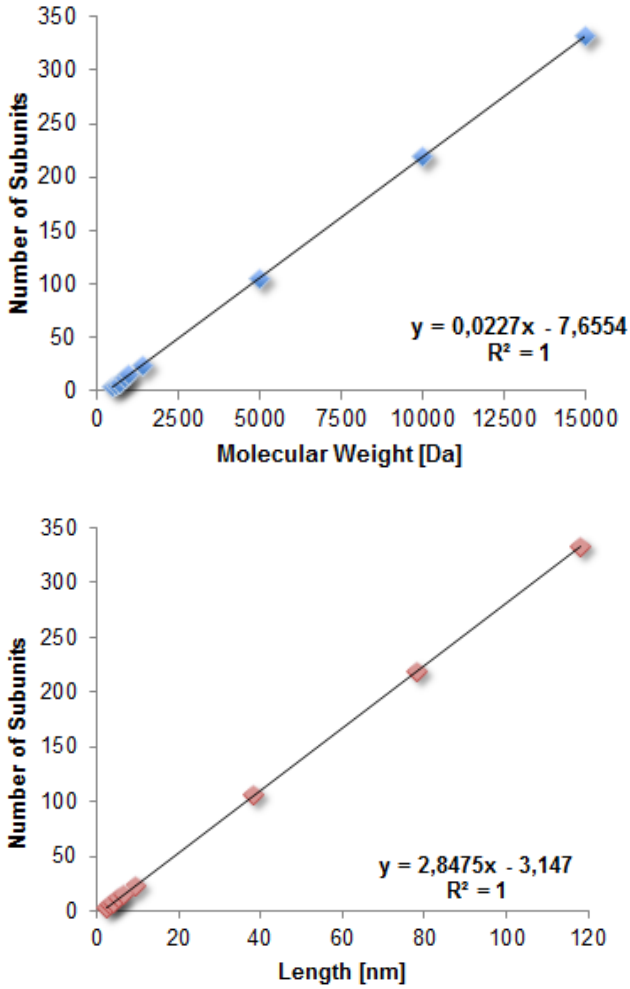

Supplemental Figure S12. Conversion of PEG molecular weights with functional end groups into their corresponding lengths. Based on the molecular weight of PEGs with functional groups maleimide and NHS, the number of subunits for various PEGs can be determined. Subsequently, the PEG contour lengths for a given number of subunits can be calculated. The data were obtained from the NHS-PEG-maleimide portfolio of Thermo Scientific and Rapp Biopolymers.

Supplemental Table S3. Overview of average molecular weight and length of PEG-Polymers. In blue are the calculated polymer sizes, in black the data the calculation is based on. Number of subunits were always round to the next integer.

Molecular Weight [Da]	**Number of Subunits**	**Length [nm]**
513.3	4	2.5
601.6	6	3.2
689.71	8	3.9
865.92	12	5.3
1394.55	24	9.5
1000	15	6.4
5000	106	38.3
10000	220	78.1
15000	333	118.0

References

(1) Ott, W.; Nicolaus, T.; Gaub, H. E.; Nash, M. A. Sequence-Independent Cloning and Post-Translational Modification of Repetitive Protein Polymers through Sortase and Sfp-Mediated Enzymatic Ligation. *Biomacromolecules* **2016**, *17*, 1330−1338.

(2) Sawano, A.; Miyawaki, A. Directed Evolution of Green Fluorescent Protein by a New Versatile PCR Strategy for Site-Directed and Semi-Random Mutagenesis. *Nucleic Acids Res.* **2000**, *28*, E78.

(3) Engler, C.; Kandzia, R.; Marillonnet, S. A One Pot, One Step, Precision Cloning Method with High Throughput Capability. *PLoS One* **2008**, *3*, e3647.

(4) Schoeler, C.; Malinowska, K. H.; Bernardi, R. C.; Milles, L. F.; Jobst, M. A.; Durner, E.; Ott, W.; Fried, D. B.; Bayer, E. A.; Schulten, K.; E, G. H.; Nash, M. A. Ultrastable Cellulosome-Adhesion Complex Tightens under Load. *Nat. Commun.* **2014**, *5*, 1–8.

(5) Anthis, N. J.; Clore, G. M. Sequence-Specific Determination of Protein and Peptide Concentrations by Absorbance at 205 Nm. *Protein Sci.* **2013**, *22*, 851–858.

(6) Gasteiger, E.; Hoogland, C.; Gattiker, A.; Duvaud, S.; Wilkins, M.; Appel, R.; Bairoch, A. Protein Identification and Analysis Tools on the ExPASy Server. *The Proteomics Protocols Handbook* **2005**, 571–607.

(7) Dietz, H.; Rief, M. Exploring the Energy Landscape of GFP by Single-Molecule Mechanical Experiments. *Proc. Natl. Acad. Sci. U. S. A.* **2004**, *101*, 16192–16197.

(8) Liu, R.; Garcia-Manyes, S.; Sarkar, A.; Badilla, C. L.; Fernández, J. M. Mechanical Characterization of Protein L in the Low-Force Regime by Electromagnetic Tweezers/evanescent Nanometry. *Biophys. J.* **2009**, *96*, 3810–3821.

(9) Walther, K. A.; Gräter, F.; Dougan, L.; Badilla, C. L.; Berne, B. J.; Fernandez, J. M. Signatures of Hydrophobic Collapse in Extended Proteins Captured with Force Spectroscopy. *Proc. Natl. Acad. Sci. U. S. A.* **2007**, *104*, 7916–7921.

(10) Kühner, F.; Gaub, H. E. Modelling Cantilever-Based Force Spectroscopy with Polymers. *Polymer* **2006**, *47*, 2555–2563.